



**HAL**  
open science

## Beyond skeletal studies: A computational analysis of nasal airway function in climate adaptation

Markus Bastir, Daniel Sanz-prieto, Manuel A Burgos, Alejandro Pérez-ramos, Yann Heuzé, Laura Maréchal, Andrej Evteev, Viviana Toro-ibacache, Francisco Esteban-ortega

### ► To cite this version:

Markus Bastir, Daniel Sanz-prieto, Manuel A Burgos, Alejandro Pérez-ramos, Yann Heuzé, et al.. Beyond skeletal studies: A computational analysis of nasal airway function in climate adaptation. American Journal of Biological Anthropology, 2024, 184 (2), pp.e24932. 10.1002/ajpa.24932 . hal-04678090

**HAL Id: hal-04678090**

<https://hal.science/hal-04678090v1>

Submitted on 26 Aug 2024

**HAL** is a multi-disciplinary open access archive for the deposit and dissemination of scientific research documents, whether they are published or not. The documents may come from teaching and research institutions in France or abroad, or from public or private research centers.

L'archive ouverte pluridisciplinaire **HAL**, est destinée au dépôt et à la diffusion de documents scientifiques de niveau recherche, publiés ou non, émanant des établissements d'enseignement et de recherche français ou étrangers, des laboratoires publics ou privés.



Distributed under a Creative Commons Attribution - NonCommercial - NoDerivatives 4.0 International License

## RESEARCH ARTICLE

# Beyond skeletal studies: A computational analysis of nasal airway function in climate adaptation

Markus Bastir<sup>1</sup>  | Daniel Sanz-Prieto<sup>1,2,3</sup>  | Manuel A. Burgos<sup>2</sup> |  
Alejandro Pérez-Ramos<sup>4</sup> | Yann Heuzé<sup>5</sup>  | Laura Maréchal<sup>5</sup> | Andrej Evteev<sup>6</sup>  |  
Viviana Toro-Ibacache<sup>7</sup>  | Francisco Esteban-Ortega<sup>8</sup>

<sup>1</sup>Paleoanthropology Group, Department of Paleobiology, National Museum of Natural Sciences-Spanish National Research Council, Madrid, Spain

<sup>2</sup>Fluid Mechanics and Thermal Engineering Group, Department of Thermal and Fluid Engineering, Polytechnic University of Cartagena, Cartagena, Spain

<sup>3</sup>Department of Biology, Faculty of Sciences, Autonomous University of Madrid, Madrid, Spain

<sup>4</sup>Paleobiology, Paleoclimatology, and Paleogeography Group, Department of Ecology and Geology, Faculty of Science, University of Málaga, Malaga, Spain

<sup>5</sup>CNRS, Ministère de la Culture, PACEA, Université de Bordeaux, Pessac, France

<sup>6</sup>Anuchin Research Institute and Museum of Anthropology, Lomonosov Moscow State University, Moscow, Russia

<sup>7</sup>Center for Quantitative Analysis in Dental Anthropology, Faculty of Dentistry, University of Chile, Santiago, Chile

<sup>8</sup>Department of Surgery, Faculty of Medicine, University of Seville, Seville, Spain

## Correspondence

Markus Bastir, Paleoanthropology Group,  
Department of Paleobiology, National  
Museum of Natural Sciences-Spanish National  
Research Council. C/Serrano 115 bis, 28006  
Madrid, Spain.  
Email: [mbastir@mncn.csic.es](mailto:mbastir@mncn.csic.es)

## Funding information

Ministerio de Ciencia e Innovación,  
Grant/Award Numbers: PID2019-105097RB-  
I00/MCIN/AEI/10.13039/50110001103,  
PID2020-115854GB-I00/MCIN/AEI/  
10.13039/50110001103

## Abstract

**Objectives:** Ecogeographic variation in human nasal anatomy has historically been analyzed on skeletal morphology and interpreted in the context of climatic adaptations to respiratory air-conditioning. Only a few studies have analyzed nasal soft tissue morphology, actively involved in air-conditioning physiology.

**Materials and Methods:** We used in vivo computer tomographic scans of ( $N = 146$ ) adult individuals from Cambodia, Chile, Russia, and Spain. We conducted ( $N = 438$ ) airflow simulations during inspiration using computational fluid dynamics to analyze the air-conditioning capacities of the nasal soft tissue in the inflow, functional, and outflow tract, under three different environmental conditions: cold-dry; hot-dry; and hot-humid. We performed statistical comparisons between populations and sexes.

**Results:** Subjects from hot-humid regions showed significantly lower air-conditioning capacities than subjects from colder regions in all the three conditions, specifically within the isthmus region in the inflow tract, and the anterior part of the internal functional tract. Posterior to the functional tract, no differences were detected. No differences between sexes were found in any of the tracts and under any of the conditions.

**Discussion:** Our statistical analyses support models of climatic adaptations of anterior nasal soft tissue morphology that fit with, and complement, previous research on

Markus Bastir and Daniel Sanz-Prieto contributed equally to this study.

This is an open access article under the terms of the [Creative Commons Attribution-NonCommercial-NoDerivs](https://creativecommons.org/licenses/by-nc-nd/4.0/) License, which permits use and distribution in any medium, provided the original work is properly cited, the use is non-commercial and no modifications or adaptations are made.

© 2024 The Authors. *American Journal of Biological Anthropology* published by Wiley Periodicals LLC.

dry skulls. However, our results challenge a morpho-functional model that attributes air-conditioning capacities exclusively to the functional tract located within the nasal cavity. Instead, our findings support studies that have suggested that both, the external nose and the intra-facial soft tissue airways contribute to efficiently warming and humidifying air during inspiration. This supports functional interpretations in modern midfacial variation and evolution.

#### KEYWORDS

air-conditioning, computational fluid dynamics, ecogeographic variation, sexual dimorphism, soft tissue

## 1 | INTRODUCTION

Morphological variation can arise from a myriad of factors such as genetic, biomechanical, or ecogeographic/climatic influences, closely related to random and nonrandom processes during evolution (Alberch, 1982; Alberch, 1990; Maynard-Smith et al., 1985). The specific influence of these factors on the variation in human craniofacial morphology is complex and not entirely understood. Nasal anatomy has been a particular focus of attention regarding its direct contact with the external environment and, consequently, for being under the influence of climatic factors, such as environmental temperature and humidity (Crognier, 1981; Davies, 1932; Proctor, 1987). Historically, many studies have investigated the relationship between climatic pressures and nasal morphology, but have mainly focused on skeletal structures (Butaric, 2015; Butaric et al., 2010; Carey & Steegmann Jr., 1981; Churchill et al., 2004; Davies, 1932; Evteev et al., 2014; Evteev & Grosheva, 2019; Franciscus, 1995; Franciscus & Long, 1991; Harvati & Weaver, 2006; Holton et al., 2013; Kelly et al., 2023; Maddux et al., 2017; Marks et al., 2019; Noback et al., 2011; Schlager & Rüdell, 2015; Thomson & Buxton, 1923; Tran & Schroeder, 2021; Weiner, 1954). It has only been in recent years that the morphological and functional study of nasal soft tissue has gained increasing relevance in evolutionary and biological anthropology (Bastir et al., 2020; Bastir et al., 2022; Heuzé, 2019; Inthavong et al., 2019; Keustermans et al., 2018; Maréchal et al., 2023; Megía et al., 2018; Ramprasad & Frank-Ito, 2016; Shah & Frank-Ito, 2022; Yokley, 2009), which does credit to its central role in respiratory physiology (Proctor & Andersen, 1982).

The nasal cavity (NC) is a complex bony structure divided by the nasal septum into two nasal fossae. The superior, middle, and inferior nasal turbinates (or conchae) are bilateral curled projections that extend from both lateral and superior walls of the NC and increase the surface area of the cavity. The superior and middle turbinates are projections stemming from the ethmoid bone, whereas the inferior turbinate is derived from its own individual center of ossification as a separate bone. The entire NC is lined with a highly vascularized respiratory mucosa that has erectile capacity in response to various stimuli (Cauna, 1982; Hopkins, 2021). This nasal mucosa undergoes cyclic and spontaneous congestions and decongestions of the nasal lumen, accompanied by shifts in nasal resistance, known as the nasal cycle

(Eccles, 1982). The “classic” nasal cycle typically presents as alternate congestions and decongestions between nasal passages, although bilateral congestions or decongestions can also occur (Grützenmacher et al., 2005).

In this article, we refer to the nasal airway (NA) as the soft tissue passages that delineate the nasal lumen through which air flows during breathing, from the nostrils (external nose) to the end of the nasopharynx, not including the paranasal sinuses (see Bastir et al., 2020; Megía et al., 2018). Previous articles have also employed the “NA” term to refer to a subset of these soft tissue passages but restricted anteriorly by the piriform aperture and posteriorly by the choanae (Heuzé, 2019; Maréchal et al., 2023).

In addition to particle filtration and olfaction, the two main physiological functions of the NA are determining the amount of air volume for gas exchange (related to respiratory energetics) and regulating the physical conditions of the inhaled and exhaled air (air-conditioning) (Sahin-Yilmaz & Naclerio, 2011). During inhalation, air-conditioning can be defined as the process by which air is modified till reaching the body core temperature and water vapor saturation to protect the lower airways from injuries and optimize gas exchange in the alveoli (Cole, 1982; Doorly et al., 2008; Elad, Wolf & Keck, 2008; Proctor, 1977; Proetz, 1951; Walker et al., 1961; Wolf et al., 2004). At the posterior end of the nasopharynx, it has been observed that the air reaches a temperature of about 31–34°C and a relative humidity (RH) of about 90%–95% in inspiration (Ingelstedt & Ivstam, 1951; Keck, Leiacker, Heinrich, et al., 2000; Keck, Leiacker, Riechelmann, & Rettinger, 2000; Lindemann et al., 2002; Naftali et al., 2005; Rouadi et al., 1999). During exhalation, air in the NAs undergo substantial cooling relative to body temperature, leading to the condensation of water vapor on the passageways, and recouping of moisture (Walker et al., 1961), a feature that may have been of particular importance in the evolution of the genus *Homo* (Franciscus & Trinkaus, 1988).

Following the inhalation physiological process, Mlynski et al. (2001) proposed an antero-posteriorly organized regionalization of the NA into three distinct morphofunctional units characterized by different airflow features. The first unit, the inflow tract, is composed of three soft-tissue anatomical structures: the nasal vestibulum; isthmus; and anterior cavum (or nasal valve). According to them, the nasal vestibulum and isthmus function as a nozzle to redirect airflow, whereas the anterior cavum serves as a diffusor. The second unit,

referred to as the functional tract, plays a crucial role in the air-conditioning process (Mlynski et al., 2001). The bilateral nasal meatuses are in this region, soft-tissue narrow passages under each bony nasal turbinate (superior, middle, and inferior) and connected by a common nasal meatus. It has been suggested that the inferior meatus accounts for around 50% of the total airflow, whereas the combined contribution to airflow of the inferior and middle meatus is approximately 80% (Kim et al., 2017; Xiong et al., 2008). The third unit, the outflow tract, is composed of the posterior cavum, choanae, and nasopharynx. In the choanae, both left and right passageways merge to direct the flow toward the lower airways.

However, it is worth noting that while the functional tract has been considered the primary area responsible for air-conditioning (e.g., Maddux et al., 2017; Mlynski et al., 2001; Noback et al., 2011), the anterior nasal segment has also been suggested to play a role in this process both during inspiration (Evtsev, 2022; Hanida et al., 2013; Inthavong et al., 2009; Keck, Leiacker, Heinrich, et al., 2000; Keck, Leiacker, Riechelmann, & Rettinger, 2000; Kumahata et al., 2010; Lindemann et al., 2002; Webb, 1951; Zhu et al., 2011) and, as mentioned previously, during expiration by moisture recouping (Franciscus & Trinkaus, 1988).

As stated above, numerous studies have addressed the climatic-mediated pressures for air-conditioning indirectly, establishing strong correlations between bony nasal morphologies and ecogeographic factors. Since cold-dry climates are most demanding in terms of breathing, the NC morphologies would have resulted in configurations that enhance the heat and moisture transfers. Thus, populations from colder and drier environments display longer, taller and narrower NC (Butaric, 2015; Churchill et al., 2004; Doorly et al., 2008; Evtsev et al., 2014; Franciscus, 1995; Franciscus & Long, 1991; Harvati & Weaver, 2006; Holton et al., 2013; Maddux et al., 2017; Schlager & Rüdell, 2015), and larger nasal turbinates (Marks et al., 2019). These morphologies would enhance the air-conditioning capacity by augmenting the ratio of mucosal surface area relative to air volume (SA/V) (Schmidt-Nielsen et al., 1970; Schroter & Watkins, 1989), as well as increasing the residence time (Inthavong et al., 2007; Noback et al., 2011) and turbulence of the airflow (Churchill et al., 2004; Cole, 2000).

In addition to the climatic influences on nasal morphology, metabolic pressures also play a significant evolutionary role (Bastir et al., 2022). The respiratory energetics hypothesis proposes that nasal dimensions are developmentally connected to the metabolic requirements for oxygen intake and was originally stated in the context of craniofacial sexual dimorphism (Enlow, 1968; Hall, 2005; Rosas & Bastir, 2002). However, it is important to note that energetics and climate are also interconnected, as climate can significantly impact metabolic demands (Froehle, 2008; Froehle et al., 2013). For instance, individuals who inhabit colder climates typically exhibit elevated basal metabolic rates compared with those in warmer regions (Leonard et al., 2005; Ocobock et al., 2021; Snodgrass et al., 2005). This is due to the additional energy requirements for thermogenesis and the maintenance of thermoregulatory advantages, such as larger or heavier bodies (Foster & Collard, 2013; Froehle et al., 2013; Ocobock et al., 2022). Thus, the respiratory energetics hypothesis has

been extended to climatic aspects with larger NC for cold environments (Bastir, 2019; Bastir & Rosas, 2013; Franciscus & Churchill, 2002; Froehle et al., 2013; Kelly et al., 2023; Maddux et al., 2017). Specifically, the respiratory-energetics hypothesis has primarily stated that metabolic influences on NC morphology may have a more direct effect on nasal heights and breadths (cross-sectional size). However, increase in breadth due to greater requirements in oxygen intake would conflict with narrower NC morphologies for improved air-conditioning in cold environments. For this reason, Maddux et al. (2017) hypothesized that the variability in both the breadth and length of nasal passages primarily relates to their air-conditioning capacity, whereas variation in height may be more related to meet metabolic requirements. This inverse interrelation between breadth and height is tentatively supported by classical ecogeographic patterns observed in nasal index (Davies, 1932; Thomson & Buxton, 1923).

Sexual dimorphism has also been extensively analyzed in relation to nasal dimensions and energetic function. Males, across different populations, consistently display larger NC than females (Bastir et al., 2011; Butaric et al., 2022; Crouse & Laine-Alava, 1999; Franciscus, 1995; Hall, 2005; Rosas & Bastir, 2002). These size differences are often attributed to the fact that males require higher volumes of air with each breath to adequately supply oxygen to their larger lungs (Torres-Tamayo et al., 2018) and more muscular bodies with greater energy demands (Bastir et al., 2011; Hall, 2005; Holton et al., 2014; Holton et al., 2016; Rosas & Bastir, 2002). Conversely, it is widely recognized that individuals inhabiting the same climatic environment should possess similar air-conditioning capacities to ensure adequate respiratory function (Franciscus, 1995; Havenith, 2005; White, 2006). Therefore, there appears to be a discrepancy between metabolic-mediated demands for larger nasal passages in males and a potential reduction in air-conditioning capacity compared with females, since the increase in size would lead to a reduction in the SA/V ratio. In this context, Kelly et al. (2023) found significant correlations between basal metabolic rates and bony nasal size in extreme cold-dry populations from Alaska, with higher metabolic demands associated with larger NC in men. They also suggested that men might compensate the loss of SA/V ratio with a longer air residence time (implying similar air-conditioning capacities between sexes), as increases in nasal height are developmentally linked to increases in nasal length (Bastir & Rosas, 2004; Enlow, 1968; Holton et al., 2011; Holton et al., 2012).

Although there is extensive literature on the NC morphology and its relation to environmental and metabolic factors, the morphofunctional study of NA is scarce. Zaidi et al. (2017) stated that the variation in the width of the nares is more differentiated across their study populations than expected under genetic drift alone. They also found that the width of the nares is correlated with environmental temperature and absolute humidity, suggesting that some aspects of the external nose may have been driven by local adaptation to climatic factors, in addition to other nonneutral evolutionary forces. Yokley (2009) observed no significant differences in the SA/V ratio individuals of European and African descent when the NA was congested but significant differences when decongested (with individuals of

European descent having higher SA/V ratio than those with African descent). Yokley (2009) also stated that climatic selection probably would be acting primarily at decongested state; hence exposure to cold would act as both decongesting and selective agent. On the other hand, Heuzé (2019) argued that a decongested NA would be more indicative of NC morphology rather than the NA itself. Utilizing a small sample from France, Heuzé (2019) found significant but low correlations between NC and NA surface areas, volumes, and SA/V ratios (when excluding the ethmoidal cells, which are more related to the olfactory function), thus urging caution in making climatic inferences from bony morphologies to soft tissue. A recent study analyzed the NA 3D shape from different geographic groups, finding subtle but significant shape differences between populations (Maréchal et al., 2023). They showed that subjects from France and Russia were the morphologically closest groups (displaying longer and narrower NAs), the Cambodian sample was the morphologically most distinct (exhibiting shorter and wider NAs), South African subjects were close to the Cambodians but also overlapped with French and Russian samples, and Chilean individuals were the most variable and dispersed. These morphological variations between NA appeared to mainly reflect genetic distances between the studied populations. Moreover, this study raised questions about the climate-related metabolic demands since they did not detect correlations between NA volume and geographic groups, suggesting the air volume intake is not affected by the NA shape variation (i.e., geographic shape differences may not be primarily driven by a metabolic functional role).

Sexual dimorphism in the NA has been explored, although not as extensively as NC morphology. Shah and Frank-Ito (2022) conducted measurements of the surface area, volume, and SA/V ratio of the NA in a small sample of people with African, Latin, East Asian, and Euro-American descents. They focused on comparisons between sexes rather than geographic groups. Their findings showed that males had significantly larger surface areas and greater volumes than females, but the SA/V ratio showed no significant difference, suggesting similar air-conditioning capacities across sexes. Bastir et al. (2020) examined sex differences in the NA 3D shape of a Spanish sample and found that males displayed taller and wider inflow tracts, taller outflow tracts, and slightly taller functional tracts. Maréchal et al. (2023) also reported larger NA volumes in males than in females. These differences are compatible with the respiratory-energetics hypothesis according to sexual dimorphism, with males requiring greater volumes of oxygen.

Experimental methods like computational fluid dynamics (CFD) can provide dynamic and functionally informative results and thus enhance our empirical and static understanding of nasal anatomy and function. Several CFD studies have explored air-conditioning in modern humans for multiple reasons, including understanding of pathological disorders (García et al., 2007), evaluating surgical outcomes quantitatively (Lindemann, Brambs, et al., 2005; Lindemann, Keck, et al., 2005; Siu et al., 2021), and investigating heat and moisture transfer to assess the effectiveness and validation of the computational methodology compared to in vivo experiments and established theory on this physiological process (Burgos et al., 2014; Hanida et al., 2013; Inthavong et al., 2009; Kim et al., 2017; Kumahata

et al., 2010). Nishimura et al. (2016) used CFD techniques to examine interspecific differences, suggesting that humans have impaired air-conditioning capacities compared to chimpanzees. However, these statistical differences may be too subtle from an evolutionary biological perspective to address adaptive consequences (Bastir et al., 2022). CFD techniques have also been employed to simulate the airflow in nasal soft tissue reconstructions of *Homo neanderthalensis* (De Azevedo et al., 2017), and *H. neanderthalensis* and *Homo heidelbergensis* (Wroe et al., 2018), who compare their results with modern humans, although their sample sizes could be considered relatively small. A CFD analysis addressing statistically experimentally yielded parameters of air-conditioning during inspiration in a large, eco-geographically diverse, and sex-balanced human sample has not been conducted yet.

Therefore, our study addresses the aforementioned gap to test the following three hypotheses:

**Hypothesis 1.** Variation in NA morphology between populations represents climatic adaptations related to air-conditioning. We hypothesize that individuals from different geographic origins (i.e., genetically diverse backgrounds) will show differences in air-conditioning capacities. Since the cold-dry environments represent the most stressful condition to respiratory function and, subsequently, the most likely to reflect selective pressures (Maddux et al., 2016), we predict that the subjects from hotter and more humid environments will have lower air-conditioning capacities than those from colder and drier regions. Considering potential significant differences among populations, we interpret lower air-conditioning capacities as lower warming in cold, lower cooling in hot, lower humidification in dry, and lower dehumidification in humid conditions.

**Hypothesis 2.** Air-conditioning capacities are not only restricted to the functional tract as defined by Mlynski et al. (2001), but also to the region anterior to it (Inthavong et al., 2009). Accordingly, we expect to find effects of air-conditioning already anterior to the functional tract in our models.

**Hypothesis 3.** Variation in NA morphology between sexes is not related to climatic factors. Therefore, we do not expect to find differences in air-conditioning capacities between males and females in any of our study populations.

## 2 | MATERIALS AND METHODS

### 2.1 | Human CT scan sample

This study is an observational retrospective analysis on 146 in vivo computer tomography (CT) scans from adult individuals with mean

age of  $42.19 \pm 14.86$  years (range from 18 to 80 years). The inclusion criteria were adulthood (>18 years) and the availability of a facial CT scan, which includes NA. The sample consisted of patients who underwent CT scans acquisition for reasons unrelated to NA diseases. One of the authors (Francisco Esteban-Ortega, ENT specialist) visually inspected the CT images to ensure the individuals did not present any abnormal anatomical features or undiagnosed conditions.

Some CT scans were part of a different study (Maréchal et al., 2023)<sup>1</sup>, of which samples from three geographic areas were available for airflow simulation: Cambodia (Phnom Penh Central Hospital), Chile (Hospital of the University of Chile in Santiago de Chile), and Russia (National Scientific and Practical Center of Children's Health in Moscow). The sample from Spain comes from the Virgen del Rocío Hospital in Sevilla and Morales Meseguer Hospital in Murcia.

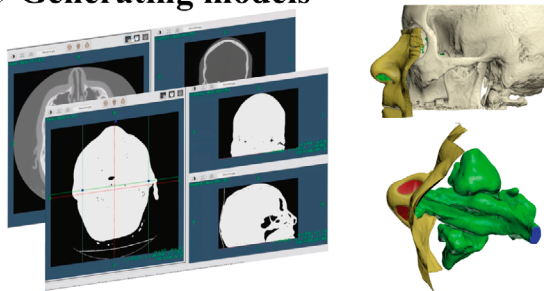
The CT images corresponded to 20 Cambodian males and 20 females, 20 Chilean males and 14 females, 15 Spanish males and 19 females, and 20 Russian males and 18 females. This study received the approval of the local Research Ethics Committees of the National Scientific and Practical Center of Children's Health and the Hospital of the University of Chile. Institutional Review Board approval was not required for data from Phnom Penh Central Hospital, or Virgen del Rocío Hospital and Morales Meseguer Hospital, considering CT scans were retrospectively selected and anonymized. Only the age and sex of the individuals were collected.

## 2.2 | Computational fluid dynamics workflow

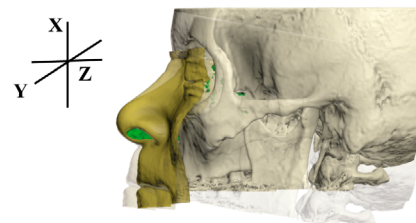
The entire CFD workflow was performed using Flowgy©, which is the fusion of preceding software (MeComLand©, DigBody© and NoseLand©) (Burgos et al., 2017; Burgos, Sanmiguel-Rojas, et al., 2018; Burgos, Sevilla-García, et al., 2018), and utilizes a CFD solver from OpenFoam® (ESI Group, 2004). The workflow consists of the following steps shown in Figure 1.

1. The CT scans were segmented to create 3D models comprising the face, NA, paranasal sinuses, and a rectangular exterior mask region (Figure 1a). The individual's craniofacial skeleton was also segmented. Three landmarks (nasion, anterior, and posterior nasal spine) were collected and used to relocate and rotate the NA 3D models to a common origin (Figure 1b), thereby ensuring a homologous position (see step 4 below). The rectangular, prismatic mask (Figure 1c) was used to identify the most "natural" air intake during inspiration, imitating an atmospheric environment. The segmentation algorithms were based on binary thresholding filters, with Hounsfield units thresholds varying between 350 and 3024.
2. The 3D models were discretized to create the computational mesh. The mesh sizes utilized in this study ranged from 7 to 15 million tetrahedral cells to ensure mesh-independent numerical outcomes (Inthavong et al., 2018). Prior studies using Flowgy© have conducted mesh convergences analyses to evaluate the precision of

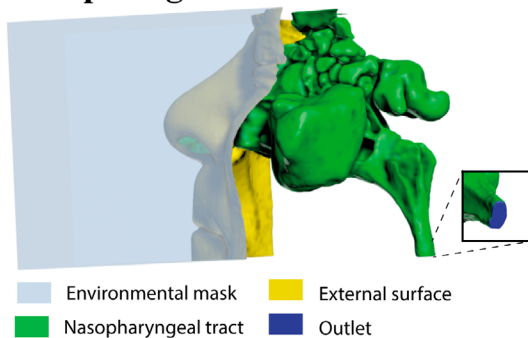
### (a) Generating models



### (b) Spatial reorientation



### (c) Computing domains



### (d) CFD study cuts

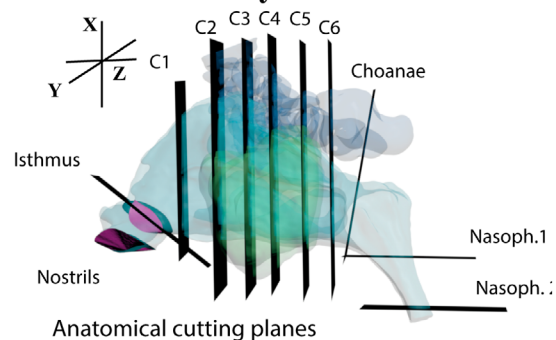


**FIGURE 1** Major steps performed during the computational fluid dynamics workflow. (a) CT data as input for segmentation of both, the craniofacial skeleton and the soft-tissue airways to generate the 3D virtual models. (b) Three landmarks, that is, nasion, the anterior, and the posterior nasal spine are used to relocate and rotate the 3D models to a common origin. (c) Computational domains comprising a prismatic exterior region, the face and the nasal airway. (d) Anatomical position of the 11 homologous cross-sectional areas along the nasal airway: nostrils and isthmus (inflow tract), six equidistant coronal cuts (functional tract), the choanae, and the two cuts in the nasopharynx (outflow tract).

CFD simulations with this software (Burgos et al., 2014; Burgos et al., *in review*).

- Airflow simulations were conducted by discretizing the Navier–Stokes equations on the computational meshes. As a boundary condition, we established an individual-specific pressure differential between the atmosphere and the nasopharynx to create a volumetric flow rate ( $Q$ ) of approximately 15 L/min. This value is commonly accepted as typical resting rate for healthy adults, as supported by previous CFD studies and physiological data (e.g., Keyhani et al., 1995; Taylor et al., 2010; Zhao & Jiang, 2014). The value of 15 L/min is also within the laminar flow range for human nasal anatomies under resting conditions, ensuring a laminar and steady flow regime (e.g., Hahn et al., 1993; Hörschler et al., 2010; Lee & Gordon, 2012; Weinhold & Mlynski, 2004; Wen et al., 2008).

All simulations were performed during one inspiratory phase, with a compressible, steady, and laminar flow. The CFD simulations accounted for aspects of NA 3D geometry. It does not take into account histological tissue differences between the external nose and those of the internal NC. A no slip boundary condition was applied to the walls. The simulations also employed rigid body dynamics to avoid deformation of soft tissues related to respiration, ensuring that the nasal anatomy does not undergo any physical changes. In our simulation models no account is taken for recouping heat and/or moisture that might have come from a previous expiration.

Three “extreme” environmental conditions were established for the outer rectangular region: cold-dry ( $-10^{\circ}\text{C}$  with a RH of 5%, i.e., an absolute humidity of  $0.11\text{ g/cm}^3$ ); hot-dry ( $40^{\circ}\text{C}$  with a RH of 5%, i.e., an absolute humidity of  $2.55\text{ g/cm}^3$ ); and hot-humid ( $40^{\circ}\text{C}$  with a RH of 85%, i.e., an absolute humidity of  $42.91\text{ g/cm}^3$ ). A cold-humid condition was not simulated since its absolute humidity values are virtually identical to cold-dry (Maddux et al., 2016). The internal nasal conditions were set at  $34^{\circ}\text{C}$ , with a RH of 95% (an absolute humidity of  $36\text{ g/cm}^3$ ), following previous CFD simulations and *in vivo* measurements (Hanida et al., 2013; Kumahata et al., 2010; Mori et al., 2015; Nishimura et al., 2016; Siu et al., 2021). In total, we conducted 438 CFD simulations.

The CFD simulations underwent post-processing and analyses. We defined 11 spatially homologous cutting planes, which intersected with the 3D NA models to determine airflow cross-sectional areas: the nostrils and the isthmus at the inflow tract (*sensu* Mlynski et al., 2001) six equidistant coronal cuts in the functional tract, the choanae, and two cuts in the nasopharynx (Figure 1d) as part of the outflow tract. The first cut in the nasopharynx was established on a plane crossing the hard palate through the anterior and posterior nasal spine. For the second, the plane included the subspinale point and transversely cut the intersection between the body and the dense of the axis (approximately the anatomical limit between the NA and the oropharynx)

The air was allowed to flow into the paranasal sinuses during the CFD simulations, but the sectors corresponding to these regions were manually erased from the cross-sectional areas. Subsequently, the means of temperature ( $^{\circ}\text{C}$ ) and absolute humidity ( $\text{g/m}^3$ ) were

extracted from each cross-sectional area to study the air-conditioning during inhalation through the NA.

It is important to consider that bilateral cutting-planes had a left and right cross-sectional area, such as the coronal cuts of the functional tract. The means of the temperature and absolute humidity were calculated of both areas to provide a single value for each anatomical section. Although we did not attempt to control for the potential morphological/physiological effects of the nasal cycle in our 3D NA models, the fact that calculating the mean of the airflow variables between both sides helps compensate for the possible presence of different stages of the “classic” asymmetric nasal cycle, with opposing effects between the left and right areas.

## 2.3 | Statistical analyses

Statistical analyses were conducted using R version 4.2.2 (R Core Team., 2022) and the ggplot2 package version 3.4.0 (Wickham, 2016) for figure creation, along with the PAST software (Hammer et al., 2001). The significance level for tests was set at  $\alpha = 0.05$ . The analyses were performed on 10 of the 11 cross-sectional areas, excluding the nostrils, which still represent ambient values of temperature and absolute humidity.

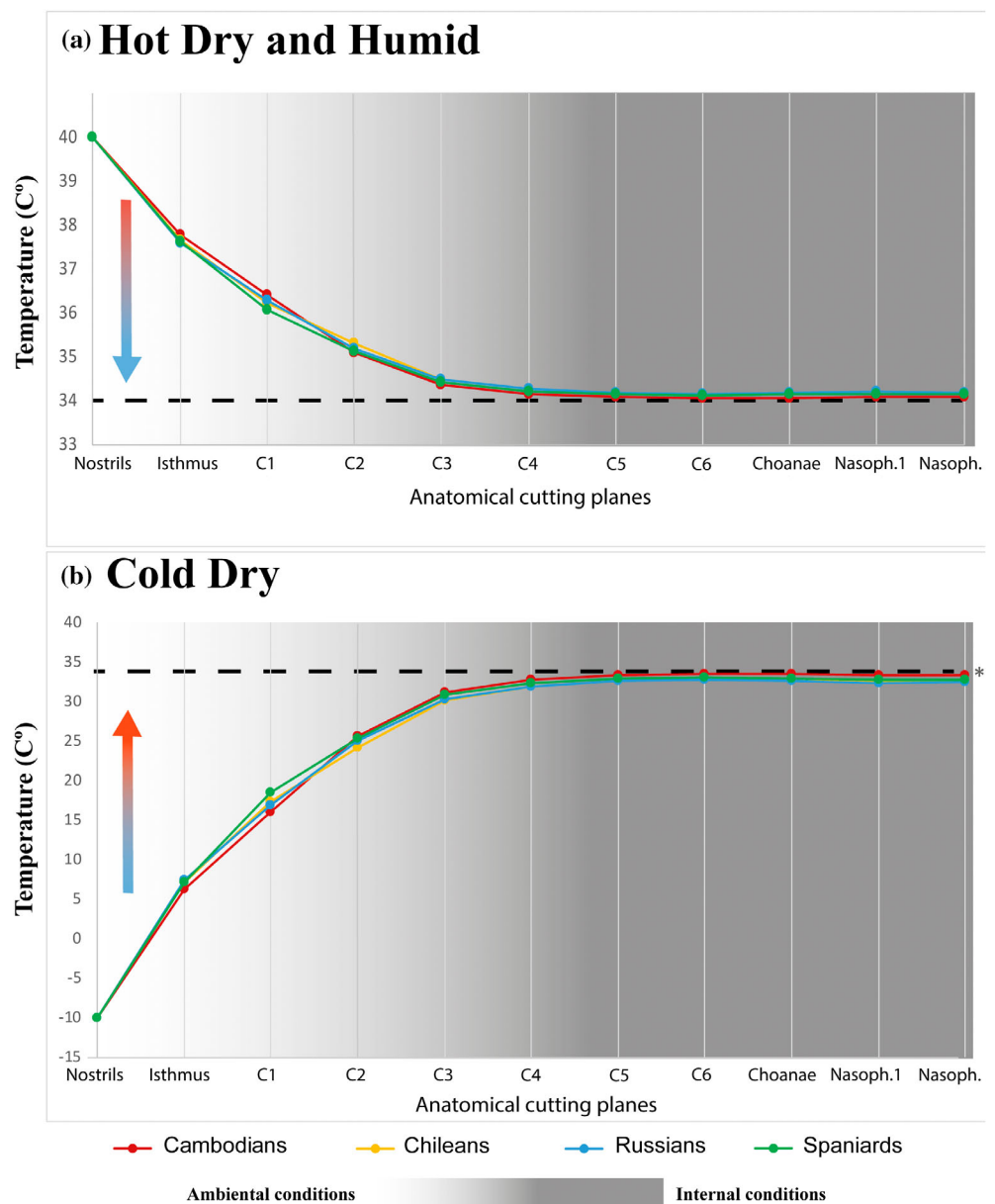
First, we analyzed the assumptions of normality (Shapiro–Wilk test) and equality of variance (Levene's test) for temperature and absolute humidity for each sex and each human population group. Based on the results of those tests, we used both parametric (*t*-tests and ANOVAs) and nonparametric approaches (Wilcoxon signed-rank and Kruskal–Wallis tests). These tests analyzed sex and geographic differences for temperature and absolute humidity. Cohen's *d* ( $d$ ), the correlation coefficient ( $r$ ), and the eta-squared ( $\eta^2$ ) were used to estimate effect sizes (Tomczak & Tomczak, 2014).

## 3 | RESULTS

### 3.1 | Geographic comparisons

Our CFD simulations indicated that Hypothesis 1 is not rejected, because the Cambodian sample showed lower warming in cold, lower cooling in hot, lower humidification in dry, and lower dehumidification in humid conditions. The means of changes due to the air-conditioning process are shown in Figure 2 for temperature and Figure 3 for humidity. Statistical comparisons of these means revealed significant geographic differences in the three environmental conditions in the isthmus and C1 (Tables 1 and 3). Post hoc analyses indicated that these differences existed between the Cambodians and the other populations (Tables 2 and 4). However, there were no significant geographic differences in temperature and absolute humidity medians at the choanae and nasopharynx for any of the environmental conditions (Tables 1 and 3). The corresponding descriptive statistics are shown in Tables S1 and S2 for temperature and Tables S3–S5 for humidity.

**FIGURE 2** Mean distributions of temperature ( $^{\circ}\text{C}$ ) by population in the nasal airway for and hot dry and humid environmental conditions (a) and for cold dry conditions (b). Note that, for the hot dry and humid conditions, the CFD simulations showed the same temperature distributions since the external and internal temperature was the same in both cases (from 40 to 34 $^{\circ}\text{C}$ ).



Hypothesis 2 is not rejected because these changes of temperature and humidity were observed both, at the isthmus level, anterior to the functional tract, and at the region of the anterior turbinates (functional tract, Tables 1–4). At the end of the NA, the inhaled air was well-conditioned in terms of temperature and absolute humidity across all human populations (Figures 2 and 3). The inhaled air was adjusted to nearly 34 $^{\circ}\text{C}$  and saturated to approximately 36 g/m $^3$  (95% RH) at the nasopharynx, even under extreme environmental conditions.

Distributions of temperature and absolute humidity are shown in Figures 4 and 5, respectively, for all populations. In the isthmus and C1, each population exhibited similar distributions for temperature and humidity (Tables S6 and S8). Also, tests of homogeneity of variance (Tables S7 and S9) found no significant differences between populations in these anatomical regions. However, toward the posterior airways, and specifically in the choanae and nasopharynx,

significant differences between populations appeared in distributions and variances. These were specifically, but not uniquely, significant between Cambodians and the rest.

### 3.2 | Sex comparisons

Figures 6 and 7 display the temperature and absolute humidity distributions, respectively, in males and females across the four human populations. Each sex exhibited similar distributions (Table S10) within the same population for both quantities, and tests of homogeneity of variance found no significant differences between sexes (Table S11). When comparing temperature (Table S1 and S2) and absolute humidity means (Table S3–S5) (isthmus, C1) and medians (choanae and nasopharynx), no significant sex differences were detected in any of the environmental conditions at any of the anatomical regions across

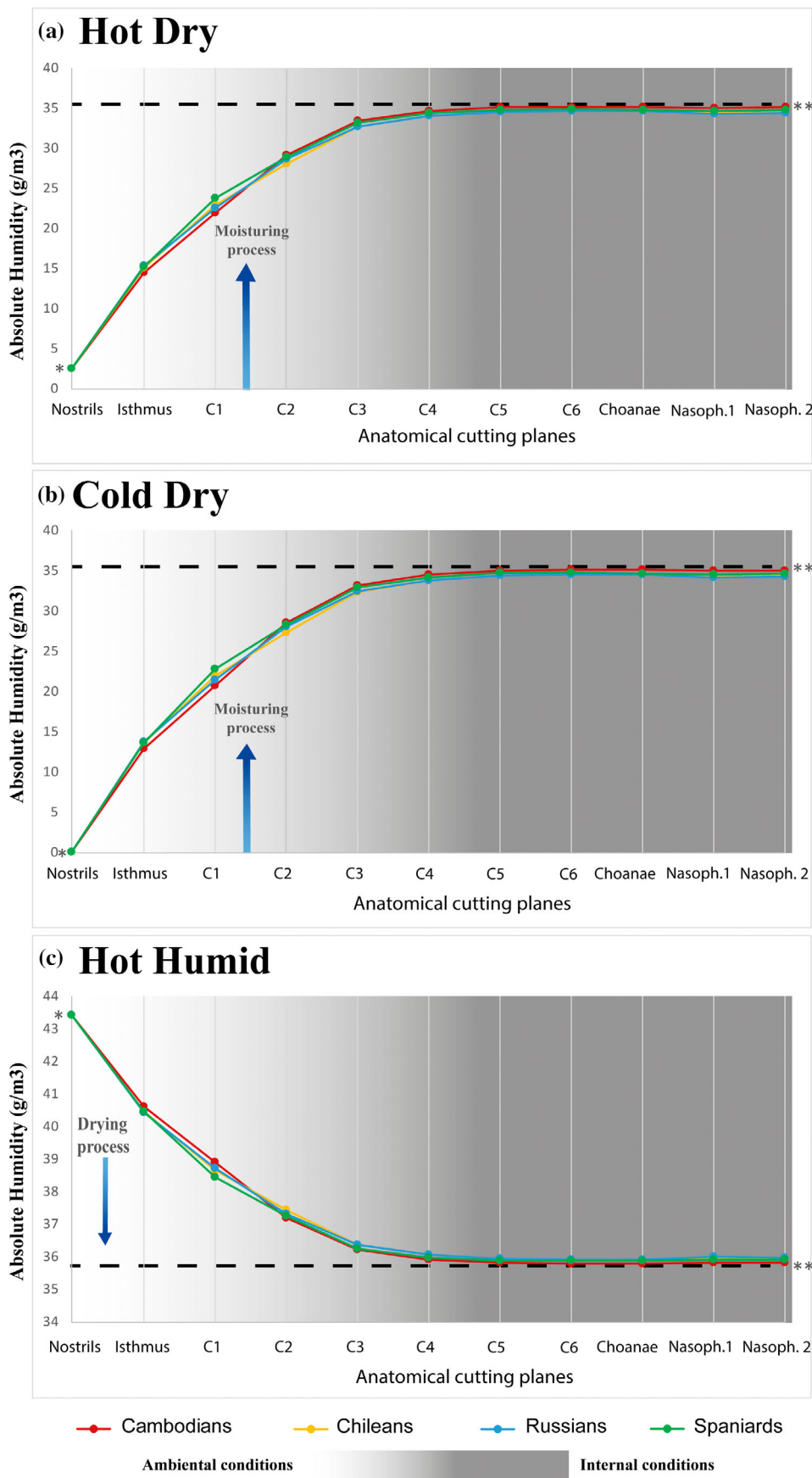


**FIGURE 3** Mean distributions of absolute humidity ( $\text{g}/\text{m}^3$ ) by population in the nasal airway for hot dry (a), cold dry (b), and hot humid environmental conditions (c).

**TABLE 1** Geographic differences for the temperature in the three environmental conditions from all the human population groups. P-values smaller than 0.05 are marked with “\*\*”.

		Isthmus	C1	C2	C3	C4	C5	C6	Choanae	Nasopharynx 1	Nasopharynx 2
Cold Dry	<i>p</i> -value	0.0032*	0.0046*	0.0844	0.1809	0.1615	0.1238	0.1302	0.0718	0.1062	0.1229
	<i>f</i> -value/ <i>h</i> -value	4.812	4.52	6.6369	4.8788	5.1449	5.7616	5.6446	7.0031	6.1136	5.779
	$\eta^2$	0.09	0.09	0.03	0.01	0.02	0.02	0.02	0.03	0.02	0.02
Hot Dry	<i>p</i> -value	0.0024*	0.0059*	0.0832	0.1863	0.1595	0.1112	0.1296	0.06548	0.1195	0.3168
	<i>f</i> -value/ <i>h</i> -value	5.027	4.334	6.6691	4.8098	5.1734	6.0095	5.6557	7.2107	5.8437	3.531
	$\eta^2$	0.10	0.08	0.03	0.01	0.02	0.02	0.02	0.03	0.02	0
Hot Humid	<i>p</i> -value	0.0024*	0.0059*	0.0832	0.1863	0.1595	0.1112	0.1296	0.0655	0.1195	0.3168
	<i>f</i> -value/ <i>h</i> -value	5.027	4.334	6.6691	4.8098	5.1734	6.0095	5.6557	7.2107	5.8437	3.531
	$\eta^2$	0.10	0.08	0.03	0.01	0.02	0.02	0.02	0.03	0.02	0

Note: ANOVAs were used in the regions that followed normal distributions, whereas Kruskal–Wallis tests were performed in the cutting planes that did not follow normal distributions.

the four populations (Tables 5 and 6). These results do not reject Hypothesis 3.

## 4 | DISCUSSION

Historically, morphological variation, and evolution in human nasal anatomy has been linked to adaptive process related to metabolic and climatic pressures (Bastir et al., 2022; Franciscus, 1995; Franciscus & Long, 1991; Franciscus & Trinkaus, 1988; Weiner, 1954). This is because primary functions of the nasal anatomy include (i) determining the intake volume of air and (ii) facilitating the respiratory air-conditioning process (Sahin-Yilmaz & Naclerio, 2011). Previous morphofunctional research has primarily relied on skeletal studies to address the climatic adaptation hypothesis, establishing correlations between specific nasal morphologies and climate variables (e. g., Carey & Steegmann Jr., 1981; Davies, 1932; Evteev et al., 2014; Maddux et al., 2017; Marks et al., 2019; Noback et al., 2011; Schlager & Rüdell, 2015; Thomson & Buxton, 1923; Weiner, 1954). However, the NC only participates indirectly in the air-conditioning process, since its dimensions define a negative space within which the NA are housed. Limited attention has been given to the NA (e. g., Bastir et al., 2020, 2022; Heuzé, 2019; Maréchal et al., 2023; Yokley, 2009), despite being the primarily responsible of heat and moisture transfer (Proctor & Andersen, 1982). The SA/V ratio has been commonly used as a proxy for air-conditioning performance, but computational simulation of fluid dynamics (CFD) can provide virtual-experimentally yielded parameters for internal temperature and humidity. Nevertheless, CFD analyses have been conducted so far only with limited sample sizes and lacking a diverse range of human variability. To bridge these gaps, the present study employs CFD simulations in three environmental conditions to address statistically the hypothesis about climatic adaptations to respiratory air-conditioning

in a large sample ( $n = 146$  subjects, 438 simulations), covering a relatively wide variety of modern human populations from four different ecogeographic areas.

Importantly, our CFD simulations detected differences in air-conditioning between the Cambodian population and the rest, occurring at the isthmus and the anterior part of the functional tract. Toward the posterior end of the NA, in the outflow tract, all populations had completely acclimatized the inhaled air (i.e., all population had similar air-conditioning capacities) in the three environmental conditions.

These findings support hypotheses about climatic adaptations of nasal morphological variation and also previous suggestions that air-conditioning is not totally restricted to the functional tract containing the turbinates (Mlynski et al., 2001), but also includes regions anterior to it (Inthavong et al., 2009). On the other hand, no sex differences were found for any of the populations and environmental conditions, supporting the previous views of similar air-conditioning capacities between sexes, despite differences in energetic needs (Bastir et al., 2020; Kelly et al., 2023; Maréchal et al., 2023).

### 4.1 | Geographic comparisons

Our primary aim was to test the hypothesis that variation in NA morphology between populations is related to climatic factors. Thus, people with disparate geographic (and thus climatic) origins would display different air-conditioning performances. Our results showed significant differences for the temperature and absolute humidity between Cambodians and the rest of sample in the isthmus, within the inflow tract and at the anterior functional tract. In turn, in the central and posterior functional tract, the choanae and in the nasopharynx (posterior to the functional tract) we did not find any differences between samples. The variances of temperature and humidity differed systematically between the Cambodian sample and Chileans and Russians.

**TABLE 2** Post hoc analyses testing temperature differences in the isthmus and C1 between human population groups. P-values smaller than 0.05 are marked with “\*\*”.

			Isthmus	C1
Cold Dry	Cambodian versus Chilean	<i>p</i> -value	0.0153*	0.0544
		<i>t</i> -value	−2.4922	−1.9574
		Cohen's <i>d</i>	0.60	0.46
	Cambodian versus Russian	<i>p</i> -value	0.0002915*	0.1897
		<i>t</i> -value	−3.7985	−1.3235
		Cohen's <i>d</i>	0.87	0.30
	Cambodian versus Spanish	<i>p</i> -value	0.0067*	0.0002*
		<i>t</i> -value	−2.7954	−3.941
		Cohen's <i>d</i>	0.67	0.92
	Chilean versus Russian	<i>p</i> -value	0.4605	0.5470
		<i>t</i> -value	−0.7426	0.60528
		Cohen's <i>d</i>	0.18	−0.14
	Chilean versus Spanish	<i>p</i> -value	0.8726	0.1042
		<i>t</i> -value	−0.16098	−1.6484
		Cohen's <i>d</i>	0.04	−0.41
Russian versus Spanish	<i>p</i> -value	0.5536	0.0234*	
	<i>t</i> -value	0.59547	−2.3191	
	Cohen's <i>d</i>	−0.14	0.55	
Hot Dry	Cambodian versus Chilean	<i>p</i> -value	0.0140*	0.0668
		<i>t</i> -value	2.5253	1.8624
		Cohen's <i>d</i>	−0.6	−0.44
	Cambodian versus Russian	<i>p</i> -value	0.0002*	0.1998
		<i>t</i> -value	3.8961	1.2938
		Cohen's <i>d</i>	−0.89	−0.3
	Cambodian versus Spanish	<i>p</i> -value	0.0062*	0.0003*
		<i>t</i> -value	2.827	3.859
		Cohen's <i>d</i>	−0.67	−0.9
	Chilean versus Russian	<i>p</i> -value	0.4228	0.5891
		<i>t</i> -value	0.80686	−0.54258
		Cohen's <i>d</i>	−0.2	0.13
	Chilean versus Spanish	<i>p</i> -value	0.8648	0.0973
		<i>t</i> -value	0.17099	1.6828
		Cohen's <i>d</i>	−0.04	−0.41
Russian versus Spanish	<i>p</i> -value	0.5194	0.0256*	
	<i>t</i> -value	−0.64773	2.281	
	Cohen's <i>d</i>	0.16	−0.54	
Hot Humid	Cambodian versus Chilean	<i>p</i> -value	0.0140*	0.0668
		<i>t</i> -value	2.5253	1.8624
		Cohen's <i>d</i>	−0.6	−0.44
	Cambodian versus Russian	<i>p</i> -value	0.0002*	0.1998
		<i>t</i> -value	3.8961	1.2938
		Cohen's <i>d</i>	−0.89	−0.3
	Cambodian versus Spanish	<i>p</i> -value	0.0062*	0.0003*
		<i>t</i> -value	2.827	3.859
		Cohen's <i>d</i>	−0.67	−0.90

TABLE 2 (Continued)

		Isthmus	C1
Chilean versus Russian	<i>p</i> -value	0.4228	0.5891
	<i>t</i> -value	0.80686	-0.54258
	Cohen's <i>d</i>	-0.2	0.13
Chilean versus Spanish	<i>p</i> -value	0.8648	0.0973
	<i>t</i> -value	0.17099	1.6828
	Cohen's <i>d</i>	-0.04	-0.41
Russian versus Spanish	<i>p</i> -value	0.5194	0.0256*
	<i>t</i> -value	-0.64773	2.281
	Cohen's <i>d</i>	0.16	-0.54

Note: T-tests were used since the temperature in this regions followed normal distributions.

TABLE 3 Geographic differences for the absolute humidity in the three environmental conditions from all the human population groups. P-values smaller than 0.05 are marked with “\*\*”.

		Isthmus	C1	C2	C3	C4	C5	C6	Choanae	Nasopharynx 1	Nasopharynx 2
Cold Dry	<i>p</i> -value	0.0022*	0.0034*	0.1031	0.1868	0.1679	0.1294	0.1306	0.0742	0.1087	0.1305
	<i>f</i> -value/ <i>h</i> -value	5.098	4.754	6.1825	4.8025	5.0542	5.6593	5.6384	6.9297	6.0597	5.640
	$\eta^2$	0.09	0.09	0.02	0.01	0.02	0.02	0.02	0.03	0.02	0.02
Hot Dry	<i>p</i> -value	0.0026*	0.0042*	0.0976	0.1903	0.1659	0.1225	0.1366	0.0699	0.1034	0.1304
	<i>f</i> -value/ <i>h</i> -value	4.966	4.599	6.3069	4.7595	5.0821	5.7868	5.5351	7.0636	6.1755	5.6426
	$\eta^2$	0.10	0.09	0.02	0.01	0.02	0.02	0.02	0.03	0.02	0.02
Hot Humid	<i>p</i> -value	0.0029*	0.0043*	0.0992	0.1848	0.1779	0.1634	0.1477	0.0887	0.1205	0.1394
	<i>f</i> -value/ <i>h</i> -value	4.881	4.588	6.27	4.8285	4.9184	5.1175	5.3534	6.5237	5.8248	5.4876
	$\eta^2$	0.09	0.09	0.02	0.01	0.01	0.02	0.02	0.03	0.02	0.02

Note: ANOVAs were used in the regions that followed normal distributions, whereas Kruskal–Wallis were performed in the cutting planes that did not follow normal distributions.

Therefore, all populations correctly acclimatized the inhaled air in the three environmental conditions, that is, they showed similar air-conditioning capacities at the end of the NA.

The Cambodian sample, our hot and humid reference population, showed lower air-conditioning capacities within the inflow tract and anterior functional tract. Skeletal studies of the past 20 years, following Mlynski et al. (2001) regionalization model, have mainly referred to the functional tract (within the NC), as the main contributor to heat and moisture exchange (e.g., Maddux et al., 2017; Noback et al., 2011). This part of the NA houses the major part of mucosa erectile tissue, histological features that are absent anterior to it. However, our results suggest that pure geometry appears to have already physiological effects on air-conditioning and fit with previous research, including both in vivo and computational studies: these stated that the anterior nasal segment is actually involved to the air-conditioning performance (Hanida et al., 2013; Inthavong et al., 2009; Keck, Leiacker, Heinrich, et al., 2000; Keck, Leiacker, Riechelmann, & Rettinger, 2000; Kumahata et al., 2010; Webb, 1951).

Franciscus and Trinkaus (1988) also suggested, although in the context of the appearance of the external nose in the evolution of the genus *Homo*, that the anterior regions of the nose may serve air-conditioning by helping recouping humidity. However, this pioneering model referred to air-conditioning during exhalation, while here we simulated only one inspiration. Future studies should extend the present simulations to considering the cyclic aspects of air conditioning.

Thus, our results support the idea that both, the inflow tract and the functional tract, contribute to the air-conditioning performance. Consequently, differences in the inflow tract would reflect the traditional morphofunctional relationships related to temperature and humidity, such as ecogeographic patterning of nasal index (Franciscus & Long, 1991; Thomson & Buxton, 1923; Weiner, 1954). The more platyrrhine noses, associated with wider and lower nasal apertures and characteristic for human populations from hotter and more humid environments, would have lower air-conditioning capacities than the more leptorrhine noses, related to narrower and taller nasal apertures and colder and drier environments. Presumably, these

**TABLE 4** Post hoc analyses testing absolute humidity differences in the isthmus and C1 between human population groups. P-values smaller than 0.05 are marked with “\*”.

			Isthmus	C1
Cold Dry	Cambodian versus Chilean	p-value	0.0079*	0.0403*
		t-value	-2.7414	-2.0904
		Cohen's d	0.66	0.50
	Cambodian versus Russian	p-value	0.0003*	0.1726
		t-value	-3.8389	-1.3771
		Cohen's d	0.88	-0.32
	Cambodian versus Spanish	p-value	0.0064*	0.0001*
		t-value	-2.8146	-4.0532
		Cohen's d	-0.67	0.95
	Chilean versus Russian	p-value	0.5777	0.4946
		t-value	-0.55968	0.68655
		Cohen's d	0.14	-0.16
	Chilean versus Spanish	p-value	0.9788	0.1204
		t-value	0.026688	-1.5744
		Cohen's d	-0.01	0.39
Russian versus Spanish	p-value	0.5426	0.0216*	
	t-value	0.61212	-2.3502	
	Cohen's d	-0.15	0.56	
Hot Dry	Cambodian versus Chilean	p-value	0.0153*	0.0516
		t-value	-2.4902	-1.9811
		Cohen's d	0.6	0.47
	Cambodian versus Russian	p-value	0.0002*	0.1814
		t-value	-3.8826	-1.3492
		Cohen's d	0.89	0.31
	Cambodian versus Spanish	p-value	0.0069*	0.0002*
		t-value	-2.7885	-3.9817
		Cohen's d	0.66	0.93
	Chilean versus Russian	p-value	0.4082	0.5540
		t-value	-0.83265	0.59459
		Cohen's d	0.2	0.14
	Chilean versus Spanish	p-value	0.8700	0.1005
		t-value	-0.16433	-1.6668
		Cohen's d	0.04	0.41
Russian versus Spanish	p-value	0.4962	0.0236*	
	t-value	0.68437	-2.3153	
	Cohen's d	-0.17	0.55	
Hot Humid	Cambodian versus Chilean	p-value	0.0157*	0.0507
		t-value	2.4796	1.9893
		Cohen's d	-0.59	-0.47
	Cambodian versus Russian	p-value	0.0002*	0.1817
		t-value	3.8634	1.3482
		Cohen's d	-0.88	-0.31
	Cambodian versus Spanish	p-value	0.0076*	0.0002*
		t-value	2.7504	3.9698
		Cohen's d	-0.65	-0.93

TABLE 4 (Continued)

		Isthmus	C1
Chilean versus Russian	p-value	0.4156	0.5472
	t-value	0.8196	-0.60497
	Cohen's d	-0.2	0.14
Chilean versus Spanish	p-value	0.8871	0.1039
	t-value	0.14254	1.6497
	Cohen's d	-0.04	-0.41
Russian versus Spanish	p-value	0.4898	0.0238
	t-value	-0.6945	2.3109
	Cohen's d	0.17	-0.55

Note: T-tests were used since the absolute humidity in this regions followed normal distributions.

anterior NA configurations are compatible with lower and higher SA/V ratio, respectively. Future studies should measure their 3D shape to fully address this assumption.

However, the absence of statistical geographic differences in the choanae and nasopharynx (outflow/post-functional tract regions) in our findings does not strictly align with the previous assumptions that variation in NC morphology represents climatic adaptations, according to which people from hotter and more humid environments would show lower air-conditioning capacities than those from colder and drier regions (Evtsev et al., 2014; Maddux et al., 2017). People from hotter and more humid environments only showed lower air-conditioning capacities at the anterior NA. To interpret these results, we refer to the three main morphofunctional strategies documented in the literature that are related to improved air-conditioning performances: increased SA/V ratio (Schmidt-Nielsen et al., 1970; Schroter & Watkins, 1989), longer residence time (Inthavong et al., 2007; Noback et al., 2011), or higher turbulence of the airflow (Churchill et al., 2004; Cole, 2000).

Regarding SA/V ratio, Maréchal et al. (2023) did not find any differences between the NA volume in their geographic groups from Cambodia, Chile, France, Russia, and South Africa. Thus, NA volume would be similar between Cambodians, Chileans, and Russians. On the other hand, they described that the NA shape in Cambodians tended to be antero-posteriorly shorter and mediolaterally wider than the other populations, which would imply a potentially lower SA/V ratio, assuming similar NA volume between these populations (see Kelly et al., 2023 to delve deeper into this geometric rationale). A differential residence time also does not appear to be a plausible explanation, considering these same trends reported by Maréchal et al. (2023). In principle, shorter NA, as were observed in the Cambodian sample, would result in a decreased residence time compared with the other populations. The residence time could be increased with higher nasal resistance; however, a recent study has found no differences in nasal resistances among Cambodians, Russians, and Spaniards (Burgos et al., in review). Thus, the last morphofunctional explanation would be that the Cambodians may possess higher turbulences in their airflows within the functional tract to compensate their potentially lower SA/V ratio and more brief residence time. This hypothesis should be addressed with CFD simulations accounting for

physical parameters (e.g., vorticity) of the airflows or employing turbulent airflow regimes.

Since the values in the nasopharynx (outflow tract) represent the physical properties of the airflow when moving toward lower airways, we find that all our populations have equally well-conditioned the inhaled air, regardless of external environmental conditions. To assert this, we focus on the mean temperature and absolute humidity of the Russian sample at the nasopharynx for the cold-dry environmental condition: 32.46°C and 34.30 g/m<sup>3</sup>, respectively (see Tables S1 and S2). These mean airflow quantities are the most distant from the established internal target conditions for the CFD simulations, with a difference of 1.54°C and 1.70 g/m<sup>3</sup>. It should be pointed out here that the air-conditioning process is not restricted just to the NA; it will continue in the lower airways before reaching the alveoli (McFadden Jr et al., 1985). The rest of populations displayed smaller differences between their means and internal conditions. Moreover, the quantities at the nasopharynx were even closer for the hot-dry and hot-humid environmental conditions in all the populations.

Indeed, there are some individuals in our sample whose temperatures and humidities are further away from those values. If our sample size was smaller and these subjects were placed outside the central tendencies that we see in the distributions (Figures 3–7), we may have found statistical differences in the outflow tract. That is why we want to emphasize the importance of studying air-conditioning with large samples. For instance, Nishimura et al. (2016) reported a mean temperature of 29.3°C before the nasopharyngeal region for their less severe cold-dry condition (5°C and 5% RH), with an inner temperature of also 34°C. Based on these results, they stated that modern humans have an impaired air-conditioning process compared to chimpanzees, although they only simulated five Japanese subjects. Although their CFD configuration model has some differences with ours, including several layers of tissues and latent heat (Hanida et al., 2013; Kumahata et al., 2010), it is possible that their findings could be unrepresentative for the human variability due to their small sample size.

Moreover, another factor to consider influencing the air-conditioning performance could be seasonality, specifically with regard to the statistically significant variances between Cambodians on the one hand, and Chileans and Russian on the other; and nearly significantly

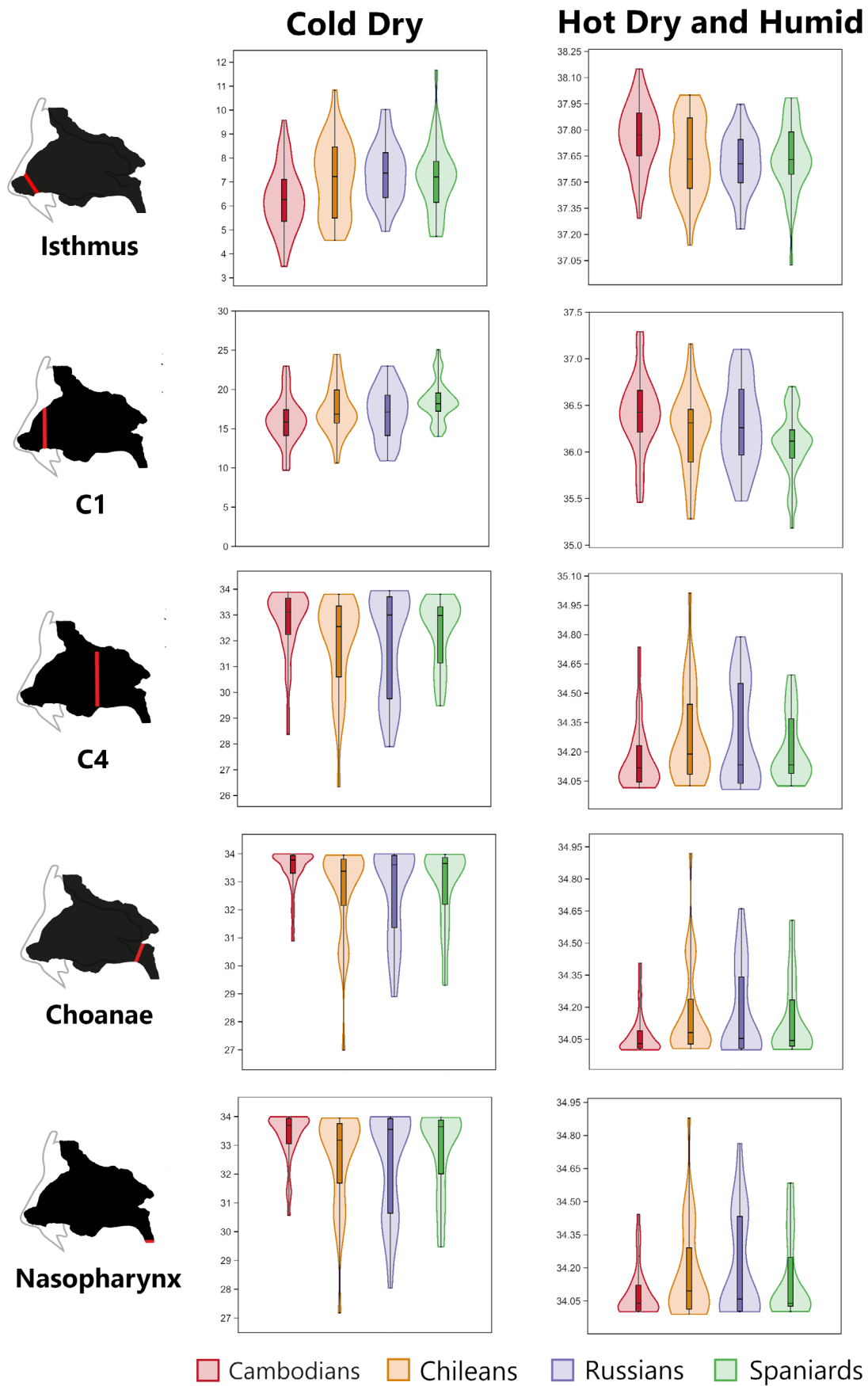


**FIGURE 4** Violin plots by population of the temperature (°C) in the isthmus, C1, C4, choanae, and nasopharynx for each environmental condition.

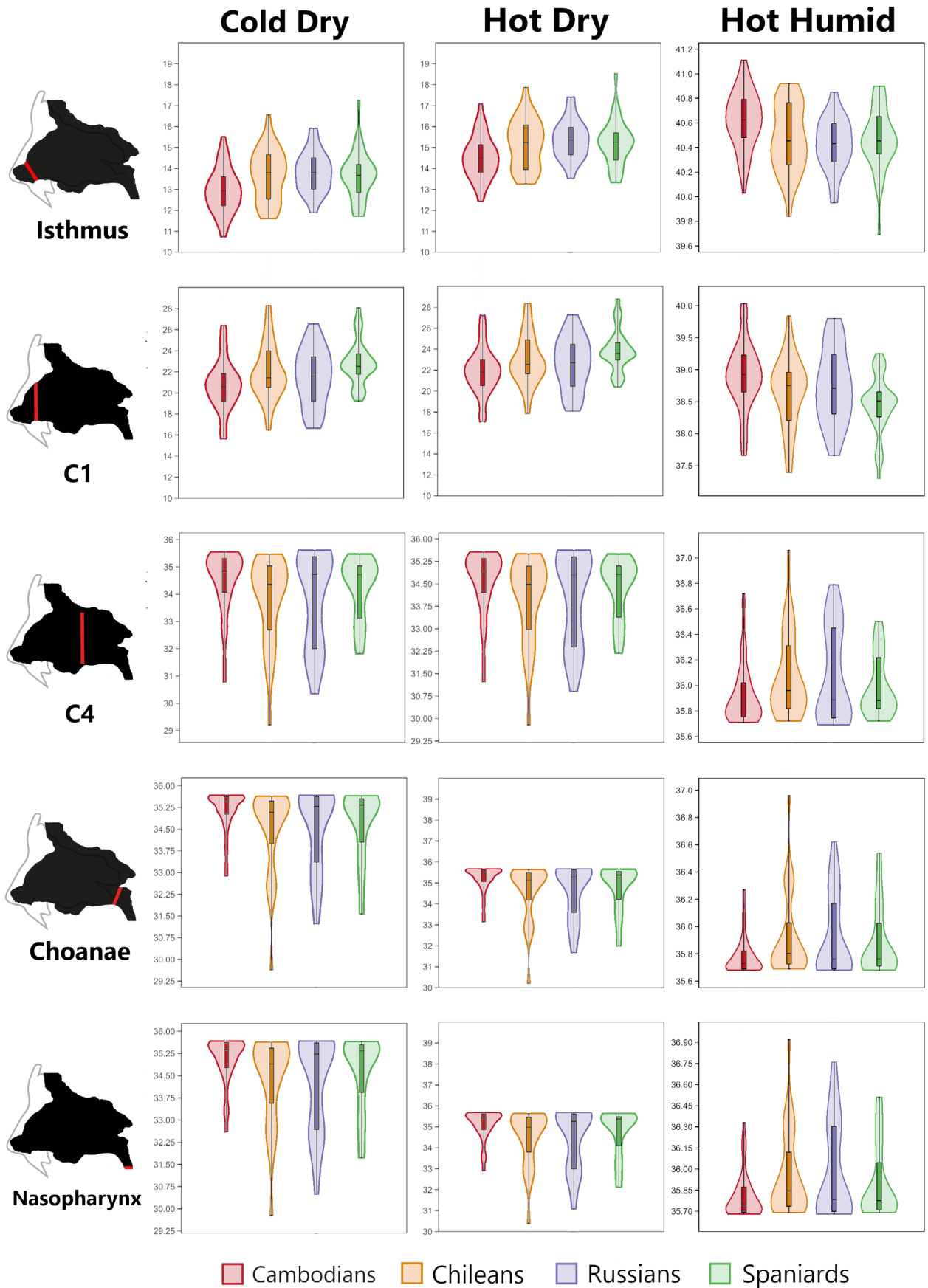


**FIGURE 5** Violin plots by population of the absolute humidity ( $\text{g}/\text{m}^3$ ) in the isthmus, C1, C4, choanae, and nasopharynx for each environmental condition.

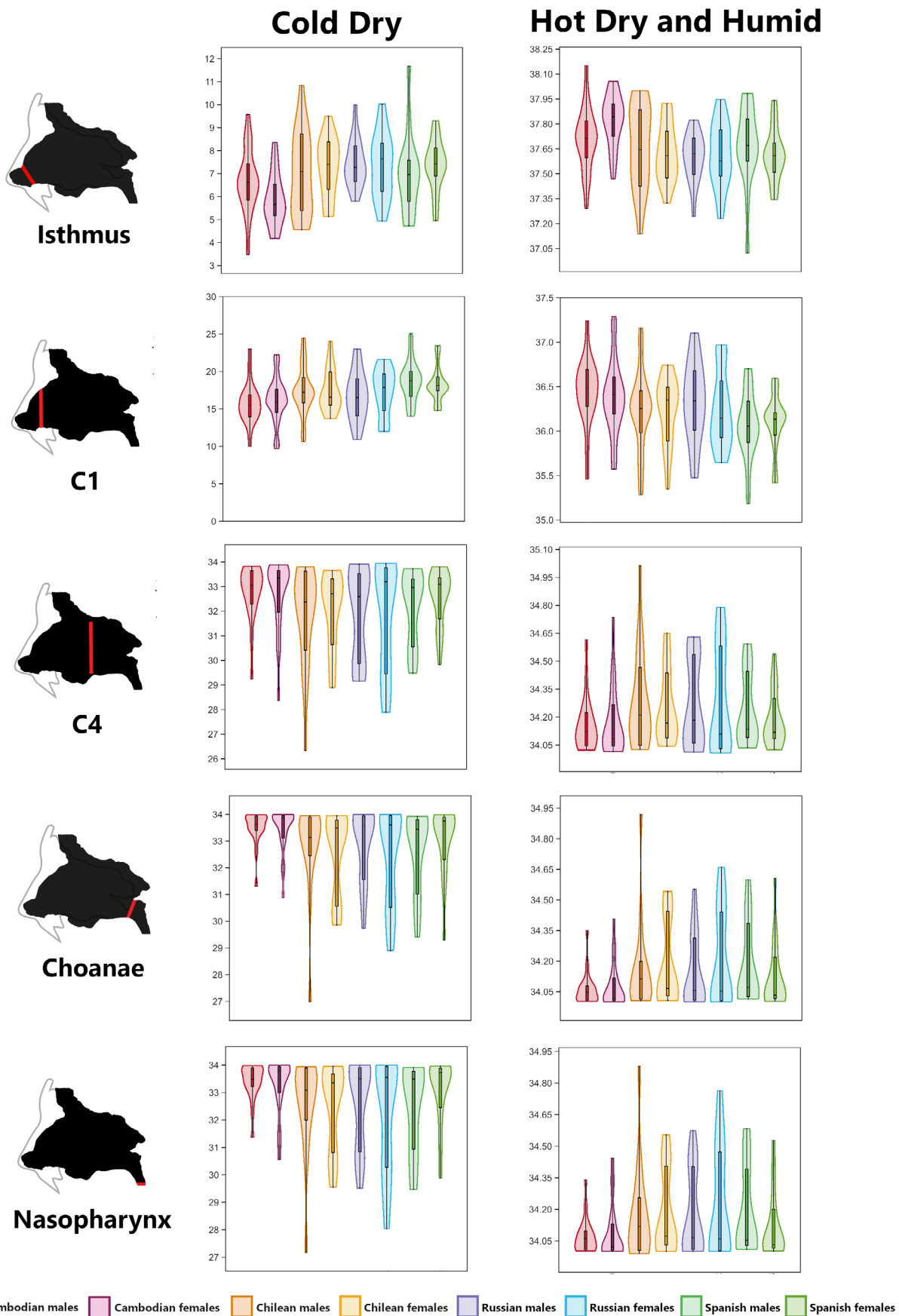


**FIGURE 6** Violin plots by sex and population of the temperature (°C) in the isthmus, C1, C4, choanae, and nasopharynx for each environmental condition.

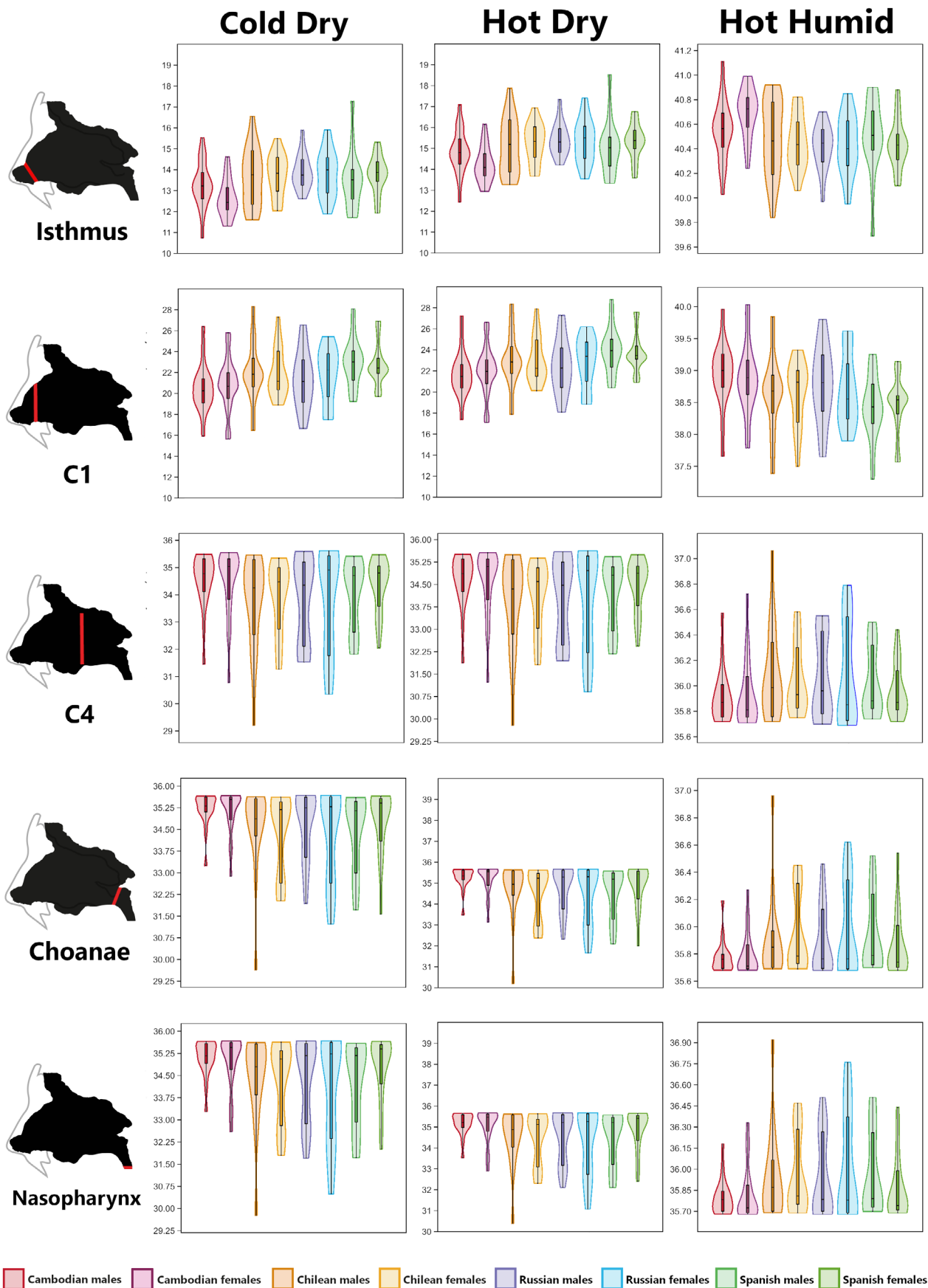


**FIGURE 7** Violin plots by sex and population of the absolute humidity ( $\text{g}/\text{m}^3$ ) in the isthmus, C1, C4, choanae, and nasopharynx for each environmental condition.

TABLE 5 Sex differences for the temperature in the three environmental conditions from the four human population groups.

		Isthmus	C1	C2	C3	C4	C5	C6	Choanae	Nasopharynx 1	Nasopharynx 2	
Cold Dry	Cambodian	p-value	0.0552	0.6169	0.4652	0.4819	0.7455	0.5162	0.7764	0.7972	0.7455	0.7049
		t-value/z-value	-1.9808	0.50438	0.73035	0.7033	0.3246	0.6492	0.28404	0.25699	0.32462	0.3787
		Cohen's d/r	0.64	0.16	0.2	0.11	0.05	0.10	0.05	0.04	0.05	0.06
	Chilean	p-value	0.6138	0.9867	0.6950	0.5232	0.9450	0.7043	0.7301	0.7562	0.7043	0.6538
		t-value/z-value	0.50985	-0.016768	0.39573	0.63836	0.069007	-0.37954	-0.34503	-0.31053	-0.37954	-0.44854
		Cohen's d/r	-0.18	0.01	-0.14	0.11	0.01	-0.07	-0.06	-0.05	-0.07	-0.08
	Russian	p-value	0.76	0.5734	0.6912	0.661	0.9185	0.9069	0.7257	0.7700	0.8493	0.8151
		t-value/z-value	-0.3082	0.5683	0.4005	0.43853	0.10233	-0.11694	-0.35082	-0.29238	-0.19004	-0.23388
		Cohen's d/r	0.10	-0.19	-0.13	0.07	0.02	-0.02	-0.06	-0.05	-0.03	-0.04
	Spanish	p-value	0.5266	0.7673	0.15	0.6416	0.4988	0.3954	0.3061	0.2822	0.1933	0.1706
		t-value/z-value	0.64325	-0.29883	-1.487	0.47075	0.67645	0.8499	1.0233	1.0755	1.3009	1.3702
		Cohen's d/r	-0.24	0.11	0.52	-0.17	0.12	0.15	0.18	0.18	0.22	0.24
Hot Dry	Cambodian	p-value	0.0525	0.6292	0.47	0.4903	0.7660	0.5337	0.8076	0.7763	0.6848	0.5072
		t-value/z-value	2.0043	-0.48686	-0.73035	-0.68984	-0.29758	-0.6223	-0.24353	-0.2842	-0.4059	-0.66313
		Cohen's d/r	-0.65	0.16	-0.12	-0.11	-0.05	-0.10	-0.04	-0.05	0.06	-0.10
	Chilean	p-value	0.6306	0.9939	0.7072	0.5809	0.9176	0.7043	0.6787	0.7430	0.6787	0.6537
		t-value/z-value	-0.48572	0.0076535	-0.40	-0.55205	-0.10351	0.37954	0.41426	0.32783	0.41423	0.44858
		Cohen's d/r	0.17	0	0.13	-0.10	-0.02	0.07	0.07	0.06	0.07	0.08
	Russian	p-value	0.7519	0.5753	0.6902	0.6610	0.9185	0.8722	0.7700	0.7588	0.8837	0.8722
		t-value/z-value	0.31892	-0.5653	-0.40184	-0.43853	-0.10233	0.16082	0.29242	0.30705	0.14623	0.16091
		Cohen's d/r	-0.11	0.19	0.13	-0.07	-0.02	0.03	0.05	0.05	0.02	0.03
	Spanish	p-value	0.5301	0.8065	0.147	0.6602	0.4769	0.3489	0.3060	0.2744	0.1992	0.2053
		t-value/z-value	-0.63763	0.24731	1.487	-0.44451	-0.7113	-0.93669	-1.0237	-1.0931	-1.2838	-1.2666
		Cohen's d/r	0.24	-0.09	-0.52	0.16	-0.12	-0.16	-0.18	-0.19	-0.22	-0.22
Hot Humid	Cambodian	p-value	0.0525	0.6292	0.47	0.4903	0.7660	0.5337	0.8076	0.7763	0.6848	0.5072
		t-value/z-value	2.0043	-0.48686	-0.73035	-0.68984	-0.29758	-0.6223	-0.24353	-0.2842	-0.4059	-0.66313
		Cohen's d/r	-0.65	0.16	-0.12	-0.11	-0.05	-0.10	-0.04	-0.05	0.06	-0.10

TABLE 5 (Continued)

	Isthmus	C1	C2	C3	C4	C5	C6	Choanae	Nasopharynx 1	Nasopharynx 2
Chilean	p-value	0.6306	0.7072	0.5809	0.9176	0.7043	0.6787	0.7430	0.6787	0.6537
	t-value/z-value	-0.48572	-0.40	-0.55205	-0.10351	0.37954	0.41426	0.32783	0.41423	0.44858
	Cohen's d/r	0.17	0.13	-0.10	-0.02	0.07	0.07	0.06	0.07	0.08
Russian	p-value	0.7519	0.6902	0.6610	0.9185	0.8722	0.7700	0.7588	0.8837	0.8722
	t-value/z-value	0.31892	-0.40184	-0.43853	-0.10233	0.16082	0.29242	0.30705	0.14623	0.16091
	Cohen's d/r	-0.11	0.13	-0.07	-0.02	0.03	0.05	0.05	0.02	0.03
Spanish	p-value	0.5301	0.147	0.6602	0.4769	0.3489	0.3060	0.2744	0.1992	0.2053
	t-value/z-value	-0.63763	1.487	-0.44451	-0.7113	-0.93669	-1.0237	-1.0931	-1.2838	-1.2666
	Cohen's d/r	0.24	-0.52	0.16	-0.12	-0.16	-0.18	-0.19	-0.22	-0.22

Note: T-tests were used in the regions that followed normal distributions, whereas Wilcoxon–Mann–Whitney tests were performed in the cutting planes that did not follow normal distributions.

different ones between Cambodians and Spaniards (Tables S6 and S10). It is important to note that the CT scans of Cambodians were obtained during the same season of the year. Also, it is worth noting that Cambodians reside in a humid and warm, tropical climate where temperatures tend to remain relatively stable throughout the year. This could be reflected in their smaller ranges of temperature and humidity variations compared with the other geographic groups, across the same anatomical regions and external environmental conditions (see SD in Tables S1 and S2). Moreover, the high absolute humidity in their environment contributes to reduced seasonal variations when compared with colder and drier climates. By contrast, the CT scans of the rest of the populations were performed throughout the year and, therefore, in different seasons and the ranges of temperature and humidity were much greater.

Therefore, seasonality may be affecting NA shape, although perhaps not strongly enough for there to be significant differences in the air-conditioning performances throughout the entire NA, but enough to be reflected in the higher temperature and humidity variances of the non-Cambodian population groups. Finally, Cambodians display smaller morphological variation than Russians and Chileans (Maréchal et al., 2023), maybe reflecting no recent admixture with other populations and indicating early genetic isolation of the population (Kloss-Brandstätter et al., 2021). A less morphologically variable NA shape would also translate into less variable air-conditioning performances within this population.

## 4.2 | Sex comparisons

Our second aim was to address the hypothesis that variation in NA morphology between sexes is not related to climatic factors, but to metabolic-mediated demands. Numerous previous studies have described the sexual dimorphism in soft and bony nasal morphologies, with males possessing larger nasal dimensions than females (Bastir et al., 2011, 2020; Bastir & Rosas, 2013; Crouse & Laine-Alava, 1999; Franciscus, 1995; Hall, 2005; Kelly et al., 2023; Maddux et al., 2017; Maréchal et al., 2023; Rosas & Bastir, 2002; Schlager & Rüdell, 2015).

We did not find sex differences in the air-conditioning process at the end of the NA for our study populations groups, a result that would align with the idea that individuals inhabiting the same climatic environment must possess similar air-conditioning capacities to ensure adequate respiratory function (Franciscus, 1995; Havenith, 2005; White, 2006). Thus, the size and shape differences between sexes in the 3D NA morphologies seem to be more compatible with the respiratory-energetics demands related to sexual dimorphism (Bastir et al., 2020; Maréchal et al., 2023). As Kelly et al. (2023) stated, there should be a developmental solution for the increase of nasal size in men without involving a sacrifice in heat/moisture transfer potential. They proposed that the loss of SA/V ratio would be compensated with greater air residence time, since nasal heights and lengths are developmentally linked. In this regard, CFD simulations accounting quantitatively the residence time would be a weightier argument for their hypothesis.

TABLE 6 Sex differences for the absolute humidity in the three environmental conditions from the four human population groups.

		Isthmus	C1	C2	C3	C4	C5	C6	Choanae	Nasopharynx 1	Nasopharynx 2	
Cold Dry	Cambodian	p-value	0.05132	0.627	0.4819	0.5792	0.7764	0.5606	0.8076	0.8710	0.7454	0.7351
		t-value/z-value	-2.0152	0.4899	0.7033	0.55455	0.28407	0.58201	0.24355	0.1624	0.32474	0.33828
		Cohen's d/r	0.65	-0.16	0.1112015	0.09	0.05	0.09	0.04	0.03	0.05	0.05
	Chilean	p-value	0.7969	0.9303	0.7312	0.6168	0.9587	0.6788	0.7169	0.7561	0.6662	0.6662
		t-value/z-value	0.25963	-0.088179	0.34655	0.50037	0.051759	-0.41413	-0.36264	-0.31062	-0.43132	-0.43136
		Cohen's d/r	-0.09	0.03	-0.12	0.09	0.01	-0.07	-0.06	-0.05	-0.07	-0.07
Russian	Russian	p-value	0.7177	0.5837	0.7063	0.6088	0.9069	0.9185	0.7366	0.7699	0.8378	0.7812
		t-value/z-value	-0.36489	0.55294	0.37983	0.51176	0.11695	-0.10233	-0.3363	-0.29246	-0.2047	-0.27781
		Cohen's d/r	0.12	-0.18	-0.13	0.09	0.02	-0.02	-0.06	-0.05	-0.04	-0.05
	Spanish	p-value	0.5482	0.7554	0.1294	0.6763	0.5209	0.4249	0.3142	0.2899	0.1815	0.1932
		t-value/z-value	0.60973	-0.31468	-1.5574	0.42207	0.642	0.79799	1.0065	1.0584	1.3361	1.3011
		Cohen's d/r	-0.23	0.11	0.55	-0.15	0.11	0.14	0.17	0.18	0.23	0.22
Hot Dry	Cambodian	p-value	0.05148	0.6369	0.4651	0.5792	0.7868	0.579	0.8181	0.9138	0.7970	0.7148
		t-value/z-value	-2.0137	0.47589	0.73042	0.55458	0.27053	0.55479	0.23003	0.10826	0.25718	0.36543
		Cohen's d/r	0.65	-0.15	0.12	0.09	0.04	0.09	0.04	0.02	0.04	0.06
	Chilean	p-value	0.6446	0.9757	0.7071	0.5928	0.8766	0.6914	0.704	0.7561	0.6915	0.5072
		t-value/z-value	0.46589	-0.030739	0.37916	0.53484	0.15528	-0.39691	-0.37991	-0.3106	-0.39688	-0.66313
		Cohen's d/r	-0.16	0.01	-0.13	0.09	0.03	-0.07	-0.07	-0.05	-0.07	-0.11
Russian	Russian	p-value	0.7298	0.5718	0.6941	0.6295	0.9069	0.9185	0.7256	0.7477	0.9069	0.7588
		t-value/z-value	-0.34847	0.57069	0.39651	0.48241	0.11696	-0.10236	-0.351	-0.32171	-0.11697	-0.3071
		Cohen's d/r	0.12	-0.19	-0.13	0.08	0.02	-0.02	-0.06	-0.06	-0.02	-0.05
	Spanish	p-value	0.5307	0.8054	0.1270	0.7019	0.4878	0.4452	0.3227	0.2820	0.2311	0.2247
		t-value/z-value	0.63673	-0.24879	-1.5674	0.38687	0.69385	0.76347	0.98896	1.0758	1.1974	1.2142
		Cohen's d/r	-0.24	0.09	0.55	-0.14	0.12	0.13	0.17	0.18	0.21	0.21
Hot Humid	Cambodian	p-value	0.05158	0.6382	0.4568	0.5699	0.8074	0.6540	0.8384	0.9133	0.7137	0.6833
		t-value/z-value	2.0127	-0.47402	-0.74405	-0.56821	-0.24373	-0.4482	-0.20392	-0.10882	-0.36685	-0.40794
		Cohen's d/r	-0.65	0.15	-0.12	-0.09	-0.04	-0.07	-0.03	-0.02	-0.06	-0.06

TABLE 6 (Continued)

	Isthmus	C1	C2	C3	C4	C5	C6	Choanae	Nasopharynx 1	Nasopharynx 2
Chilean	p-value	0.6433	0.7089	0.6047	0.9175	0.6660	0.7690	0.7167	0.6786	0.6409
	t-value/z-value	-0.4678	-0.37675	-0.51771	-0.10357	0.43159	0.29368	0.36284	0.41442	0.46644
	Cohen's d/r	0.16	0.13	-0.09	-0.02	0.07	0.05	0.06	0.07	0.08
Russian	p-value	0.7377	0.7049	0.6398	0.9883	0.8605	0.7246	0.7468	0.7694	0.7141
	t-value/z-value	0.33792	-0.38169	-0.46797	0.014631	0.17571	0.35227	0.32292	0.29319	0.36632
	Cohen's d/r	-0.11	0.13	-0.08	0	0.03	0.06	0.06	0.05	0.06
Spanish	p-value	0.5408	0.1292	0.7036	0.5321	0.4241	0.3572	0.3304	0.2814	0.3136
	t-value/z-value	-0.62099	1.558	-0.38455	-0.6248	-0.79927	-0.92069	-0.97332	-1.0771	-1.0078
	Cohen's d/r	0.23	-0.55	0.14	-0.11	-0.14	-0.16	-0.17	-0.18	-0.17

Note: T-tests were used in the regions that followed normal distributions, whereas Wilcoxon–Mann–Whitney tests were performed in the cutting planes that did not follow normal distributions.

### 4.3 | Limitations

We recognize some limitations and bias in our sample composition as well as related to the computer simulation of the biological air conditioning process itself. The location where the patients were scanned does not offer direct evidence regarding their geographic and genetic background. Consequently, it is important to acknowledge that our samples may exhibit heterogeneity. The relative age modernity of the sample, which theoretically could imply a higher degree of admixture, may also affect the replication of this study.

The use of CT scans also holds significant implications concerning the nasal cycle, since these images represent a snapshot of an individual at the time of being scanned. Both asymmetric and bilateral nasal cycle affect NA morphology (Yokley, 2009) and, consequently, the air-conditioning performance (Patel et al., 2015). However, for the “classic” asymmetric nasal cycle, simulating both nasal passages and doing the mean of temperature and absolute humidity between the two cross-sectional areas could help compensate for its effect. Furthermore, a recent study found no significant differences among the Cambodian, Spanish, and Russian populations examined in this work regarding nasal flow asymmetry between left and right passages and bilateral nasal resistance (Burgos et al., *in review*). Both findings, if considered as proxies for both asymmetric and bilateral nasal cycles, would indicate comparable moments of congestion–decongestion across populations.

Additionally, factors such as lifestyle medical history, and air quality could potentially influence NA morphology. However, controlling for these aspects falls beyond the scope of our study. Furthermore, there are other environmental factors, such as altitude or the temperature at which the individuals were scanned in the hospital, that we were unable to observe and can also impact NA morphology.

Finally, it is important to consider that the air-conditioning process is more complex than simulating inspiration only and focusing on nasal morphology (geometry) alone. Breathing is a cyclical process and as a previous expiration affects the subsequent inspiration from a biomechanical point of lung ventilation (Gómez-Recio et al., 2022, *in review*), previous expiration also affects the subsequent inspiration from an air-conditioning point of view (Franciscus & Trinkaus, 1988). This is not only related to 3D anatomy but also to physiology and histology (Sahin-Yilmaz & Naclerio, 2011), which is not considered in the present model.

It is known that during inhalation, the mucosal tissue in the nose provides part of its arterial blood-supplied heat as well mucosal moisture to inhaled air. However, this loss of moisture and heat is then recovered to some degree by the nose during expiration as the moisture and heat-laden air from the lungs is redeposited to an extent back onto the mucosa, which was cooled and gave up moisture in the inspiration phase. Particularly in cold–dry and hot–dry ambient conditions, this expiratory phase of recouping is important because in its absence, the nasal mucosa would lose too much heat and moisture (in cold–dry environments) and too much moisture in (hot–dry environments) to remain functionally viable (Franciscus & Trinkaus, 1988;

Walker et al., 1961). In our CFD simulation model, we only consider 3D anatomy of the soft tissues in a large comparative sample. To assess the degree, to which this dynamic would alter the finding reported here, requires the development of a more complex CFD model, a necessary future step.

However, in a field that so far has considered mostly skeletal data and speculations about functional implications, clearly, our statistical comparisons of CFD simulations are a step forward. Nevertheless, future work should also attempt to imply modeling further physiological factors, such as histological tissue differences and their functional impact on respiratory physiology (Jafek, 1983; Sahin-Yilmaz & Naclerio, 2011). For example, it is known that the thin, stratified squamous epithelium at the external nose changes gradually into the respiratory mucous membrane of the nasal passages, which corresponds to those regions, that, by 3D geometry, indicate most notable changes in humidity and temperature in air flow in our CFD models (Tables 3 and 4). Also, anterior nasal glands within the vestibulum contribute to moisturizing (Sahin-Yilmaz & Naclerio, 2011), which is probably why different populations may resolve anatomical air-conditioning problems differently following a principle of equifinality (Evteev, 2022). This researcher suggested air-conditioning capacities in regions anterior to the internal airways in certain populations and conditions highlighting the potential effect of the transitional segment of the mucosa (anterior to the functional tract), where also the most anterior goblet cells are located (Jafek, 1983; Sahin-Yilmaz & Naclerio, 2011), and which is comprised of stratified squamous epithelial cells and extends over the anterior ends of the functional tract, that is, the inferior and middle turbinates. Our findings suggest therefore that further improvements of CFD simulations should consider a combination of both, the 3D morphology (geometry) and the histology when modeling air-conditioning. The similarity of our findings to those of Inthavong et al. (2009) likely relates to a CFD model that does not consider histological differences between the inflow and the functional tract. But in future studies, this more complex model should also be applied to those populations that have inhabited the most extreme ranges of climatic variability, and their historical ancestral source populations, to test models of equifinality.

## 5 | CONCLUSIONS

The detection of variations in air-conditioning capacities within the anterior nasal region supports previous suggestions and may expand our notion of a “functional” tract slightly. The use of soft-tissue structures and employing computational methodologies can be used to complement classical “correlational” methods. However, the cyclicity of the respiratory process and histological evidence need to be implemented to improve future CFD-simulation methods. Future computational studies should also continue to implement even larger and more diverse samples, and specifically comparative samples of genetically close groups living in more variable environments to fully address the climatic adaptation hypothesis in nasal anatomy.

## AUTHOR CONTRIBUTIONS

**Markus Bastir:** Conceptualization (lead); formal analysis (equal); funding acquisition (lead); investigation (equal); methodology (supporting); writing – original draft (equal); writing – review and editing (equal). **Daniel Sanz-Prieto:** Conceptualization (lead); formal analysis (lead); investigation (equal); methodology (equal); software (supporting); writing – original draft (lead); writing – review and editing (equal). **Manuel A. Burgos:** Conceptualization (lead); formal analysis (equal); funding acquisition (lead); investigation (equal); methodology (lead); resources (equal); software (lead); writing – original draft (equal); writing – review and editing (equal). **Alejandro Pérez-Ramos:** Conceptualization (equal); formal analysis (supporting); investigation (supporting); methodology (supporting); writing – original draft (equal); writing – review and editing (equal). **Yann Heuzé:** Formal analysis (supporting); investigation (supporting); resources (equal); writing – original draft (supporting); writing – review and editing (equal). **Laura Maréchal:** Formal analysis (supporting); investigation (supporting); resources (equal); writing – original draft (supporting); writing – review and editing (equal). **Andrej Evteev:** Formal analysis (supporting); investigation (supporting); resources (equal); writing – original draft (supporting); writing – review and editing (equal). **Viviana Toro-Ibacache:** Formal analysis (supporting); investigation (supporting); resources (equal); writing – original draft (supporting); writing – review and editing (equal). **Francisco Esteban-Ortega:** Formal analysis (supporting); investigation (supporting); resources (equal); writing – original draft (supporting); writing – review and editing (supporting).

## ACKNOWLEDGMENTS

Laura Maréchal and Yann Heuzé benefited from the scientific framework of the University of Bordeaux's IdEx “Investments for the Future” program/GPR “Human Past”. Manuel A. Burgos is the developer of Flowgy©. No other conflicts of interest exist, nor financial disclosure reported. We appreciate the highly constructive feedback of anonymous reviewers on a previous version of this manuscript.

## DATA AVAILABILITY STATEMENT

The data that support the findings of this study are available upon reasonable request from the corresponding author. The data are not publicly available due to privacy or ethical restrictions.

## ORCID

Markus Bastir  <https://orcid.org/0000-0002-3141-3401>

Daniel Sanz-Prieto  <https://orcid.org/0000-0001-9003-0075>

Yann Heuzé  <https://orcid.org/0000-0002-0660-9613>

Andrej Evteev  <https://orcid.org/0000-0002-6254-1203>

Viviana Toro-Ibacache  <https://orcid.org/0000-0003-2265-8180>

## ENDNOTE

<sup>1</sup> The South African sample, utilized in Maréchal et al. (2023), was specifically obtained with permission for studies related to Maréchal's thesis. Unfortunately, due to permissions granted only for the scope of that particular thesis, we were unable to incorporate this sample in the present CFD-based study.

## REFERENCES

- Alberch, P. (1982). Developmental constraints in evolutionary processes. In J. T. Bonner (Ed.), *Evolution and development* (pp. 313–332). Springer-Verlag. [https://doi.org/10.1007/978-3-642-45532-2\\_15](https://doi.org/10.1007/978-3-642-45532-2_15)
- Alberch, P. (1990). Natural selection and developmental constraints: External versus internal determinants of order in nature. In C. J. de Rousseau (Ed.), *Primate life history and evolution* (pp. 15–35). Wiley-Liss.
- Bastir, M. (2019). Big choanae, larger face: Scaling patterns between cranial airways in modern humans and African apes and their significance in middle and late Pleistocene hominin facial evolution. *Bulletins et Mémoires de la Société d'Anthropologie de Paris*, 31(1–2), 5–13. <https://doi.org/10.3166/bmsap-2019-0055>
- Bastir, M., Godoy, P., & Rosas, A. (2011). Common features of sexual dimorphism in the cranial airways of different human populations. *American Journal of Physical Anthropology*, 146(3), 414–422. <https://doi.org/10.1002/ajpa.21596>
- Bastir, M., Megía, I., Torres-Tamayo, N., García-Martínez, D., Piqueras, F. M., & Burgos, M. (2020). Three-dimensional analysis of sexual dimorphism in the soft tissue morphology of the upper airways in a human population. *American Journal of Physical Anthropology*, 171(1), 65–75. <https://doi.org/10.1002/ajpa.23944>
- Bastir, M., & Rosas, A. (2004). Facial heights: Evolutionary relevance of postnatal ontogeny for facial orientation and skull morphology in humans and chimpanzees. *Journal of Human Evolution*, 47(5), 359–381. <https://doi.org/10.1016/j.jhevol.2004.08.009>
- Bastir, M., & Rosas, A. (2013). Cranial airways and the integration between the inner and outer facial skeleton in humans. *American Journal of Physical Anthropology*, 152(2), 287–293. <https://doi.org/10.1002/ajpa.22359>
- Bastir, M., Sanz-Prieto, D., & Burgos, M. A. (2022). Three-dimensional form and function of the nasal cavity and nasopharynx in humans and chimpanzees. *The Anatomical Record*, 305(8), 1962–1973. <https://doi.org/10.1002/ar.24790>
- Burgos, M., Sanz-Prieto, D., Bastir, M., Pérez-Ramos, A., Heuzé, Y., Maréchal, L., & Esteban-Ortega, F. (in review). *Assessment of sex and geographic differences in dimensionless parameters for human nasal airflow*. Medical & Biological Engineering & Computing.
- Burgos, M. A., Sanmiguel-Rojas, E., Del Pino, C., Sevilla-García, M. A., & Esteban-Ortega, F. (2017). New CFD tools to evaluate nasal airflow. *European Archives of Oto-Rhino-Laryngology*, 274, 3121–3128. <https://doi.org/10.1007/s00405-017-4611-y>
- Burgos, M. A., Sanmiguel-Rojas, E., Martín-Alcántara, A., & Hidalgo-Martínez, M. (2014). Effects of the ambient temperature on the airflow across a Caucasian nasal cavity. *International Journal for Numerical Methods in Biomedical Engineering*, 30(3), 430–445. <https://doi.org/10.1002/cnm.2616>
- Burgos, M. A., Sanmiguel-Rojas, E., Singh, N., & Esteban-Ortega, F. (2018). DigBody®: A new 3D modeling tool for nasal virtual surgery. *Computers in Biology and Medicine*, 98, 118–125. <https://doi.org/10.1016/j.combiomed.2018.05.016>
- Burgos, M. A., Sevilla-García, M. A., Sanmiguel-Rojas, Del Pino, C., Fernández-Vélez, C., Piqueras, F., & Esteban-Ortega, F. (2018). Virtual surgery for patients with nasal obstruction: Use of computational fluid dynamics (MeComLand®, Digbody® & Noseland®) to document objective flow parameters and optimise surgical results. *Acta Otorrinolaringologica (English Edition)*, 69(3), 125–133. <https://doi.org/10.1016/j.otoeng.2017.05.001>
- Butaric, L. N. (2015). Differential scaling patterns in maxillary sinus volume and nasal cavity breadth among modern humans. *The Anatomical Record*, 298(10), 1710–1721. <https://doi.org/10.1002/ar.23182>
- Butaric, L. N., McCarthy, R. C., & Broadfield, D. C. (2010). A preliminary 3D computed tomography study of the human maxillary sinus and nasal cavity. *American Journal of Physical Anthropology*, 143(3), 426–436. <https://doi.org/10.1002/ajpa.21331>
- Butaric, L. N., Nicholas, C. L., Kravchuk, K., & Maddux, S. D. (2022). Ontogenetic variation in human nasal morphology. *The Anatomical Record*, 305(8), 1910–1937. <https://doi.org/10.1002/ar.24760>
- Carey, J. W., & Steegmann, A. T., Jr. (1981). Human nasal protrusion, latitude, and climate. *American Journal of Physical Anthropology*, 56(3), 313–319. <https://doi.org/10.1002/ajpa.1330560312>
- Cauna, N. (1982). Blood and nerve supply to the nasal lining. In D. F. Proctor & I. B. Anderson (Eds.), *The nose: Upper airway physiology and the atmospheric environment* (pp. 45–69). Elsevier Biomedical Press BV.
- Churchill, S. E., Shackelford, L. L., Georgi, J. N., & Black, M. T. (2004). Morphological variation and airflow dynamics in the human nose. *American Journal of Human Biology*, 16(6), 625–638. <https://doi.org/10.1002/ajhb.20074>
- Cole, P. (1982). Upper respiratory airflow. In D. F. Proctor & I. B. Anderson (Eds.), *The nose: Upper airway physiology and the atmospheric environment* (pp. 163–189). Elsevier Biomedical Press BV.
- Cole, P. (2000). Biophysics of nasal airflow: A review. *American Journal of Rhinology*, 14(4), 245–250. <https://doi.org/10.2500/105065800779954383>
- Crognier, E. (1981). The influence of climate on the physical diversity of European and Mediterranean populations. *Journal of Human Evolution*, 10(8), 611–614. [https://doi.org/10.1016/S0047-2484\(81\)80069-3](https://doi.org/10.1016/S0047-2484(81)80069-3)
- Crouse, U., & Laine-Alava, M. T. (1999). Effects of age, body mass index, and gender on nasal airflow rate and pressures. *The Laryngoscope*, 109(9), 1503–1508. <https://doi.org/10.1097/00005537-199909000-00027>
- Davies, A. (1932). A re-survey of the morphology of the nose in relation to climate. *The Journal of the Royal Anthropological Institute of Great Britain and Ireland*, 62, 337–359. <https://doi.org/10.2307/2843962>
- De Azevedo, S., González, M. F., Cintas, C., Ramallo, V., Quinto-Sánchez, M., Márquez, F., Hünemeir, T., Paschetta, C., Ruderman, A., Navarro, P., Pazos, B. A., Silva de Cerqueira, C. C., Velan, O., Ramírez-Rozzi, F., Calvo, N., Castro, H. G., Paz, R. R., & González-José, R. (2017). Nasal airflow simulations suggest convergent adaptation in Neanderthals and modern humans. *Proceedings of the National Academy of Sciences*, 114(47), 12442–12447. <https://doi.org/10.1073/pnas.1703790114>
- Doorly, D. J., Taylor, D. J., & Schroter, R. C. (2008). Mechanics of airflow in the human nasal airways. *Respiratory Physiology & Neurobiology*, 163(1–3), 100–110. <https://doi.org/10.1016/j.resp.2008.07.027>
- Eccles, R. (1982). Neurological and pharmacological considerations. In D. F. Proctor & I. B. Anderson (Eds.), *The nose: Upper airway physiology and the atmospheric environment* (pp. 191–214). Amsterdam: Elsevier Biomedical Press BV.
- Elad, D., Wolf, M., & Keck, T. (2008). Air-conditioning in the human nasal cavity. *Respiratory Physiology & Neurobiology*, 163(1–3), 121–127. <https://doi.org/10.1016/j.resp.2008.05.002>
- Enlow, D. H. (1968). *The human face. An account of the postnatal growth and development of the craniofacial skeleton*. Harper & Row.
- ESI Group. (2004). OpenFOAM®-Official home of the open source computational fluid dynamics (CFD) toolbox. Retrieved from <https://www.openfoam.com/>
- Evteev, A. (2022). Toward a non-contradictory explanation of the climate-related variation of the nasal cavity and mid-face. *Moscow University Anthropology Bulletin*, 2(2022), 78–84. <https://doi.org/10.32521/2074-8132.2022.2.078-084>
- Evteev, A., Cardini, A. L., Morozova, I., & O'Higgins, P. (2014). Extreme climate, rather than population history, explains mid-facial morphology of northern Asians. *American Journal of Physical Anthropology*, 153(3), 449–462. <https://doi.org/10.1002/ajpa.22444>
- Evteev, A., & Grosheva, A. N. (2019). Nasal cavity and maxillary sinuses form variation among modern humans of Asian descent. *American Journal of Physical Anthropology*, 169(3), 513–525. <https://doi.org/10.1002/ajpa.23841>

- Foster, F., & Collard, M. (2013). A reassessment of Bergmann's rule in modern humans. *PLoS One*, 8(8), e72269. <https://doi.org/10.1371/journal.pone.0072269>
- Franciscus, R. G. (1995). *Later Pleistocene nasofacial variation in western Eurasia and Africa and modern human origins*. The University of New Mexico.
- Franciscus, R. G., & Churchill, S. E. (2002). The costal skeleton of Shanidar 3 and a reappraisal of Neandertal thoracic morphology. *Journal of Human Evolution*, 42(3), 303–356. <https://doi.org/10.1006/jhev.2001.0528>
- Franciscus, R. G., & Long, J. C. (1991). Variation in human nasal height and breadth. *American Journal of Physical Anthropology*, 85(4), 419–427. <https://doi.org/10.1002/ajpa.1330850406>
- Franciscus, R. G., & Trinkaus, E. (1988). Nasal morphology and the emergence of *Homo erectus*. *American Journal of Physical Anthropology*, 75, 517–527. <https://doi.org/10.1002/ajpa.1330750409>
- Froehle, A. W. (2008). Climate variables as predictors of basal metabolic rate: New equations. *American Journal of Human Biology*, 20(5), 510–529. <https://doi.org/10.1002/ajhb.20769>
- Froehle, A. W., Yokley, T. R., & Churchill, S. E. (2013). Energetics and the origin of modern humans. In F. H. Smith & J. C. M. Ahern (Eds.), *The origins of modern humans* (pp. 285–320). John Wiley & Sons, Inc. <https://doi.org/10.1002/9781118659991.ch8>
- García, G. J., Baillie, N., Martins, D. A., & Kimbell, J. S. (2007). Atrophic rhinitis: A CFD study of air conditioning in the nasal cavity. *Journal of Applied Physiology*, 103(3), 1082–1092. <https://doi.org/10.1152/jappphysiol.01118.2006>
- Gómez-Recio, M., González-Ruiz, J.M., Rueda, J., F. San Juan, A., Navarro, E., Beyer, B., Bastir, M., Geometric morphometrics of 4D motion data: A proof of concept for applications in palaeoanthropology. *Spanish Journal of Paleontology* 37(2):2022; 141–152. <https://doi.org/10.7203/sjp.25648>
- Grützenmacher, S., Lang, C., Mlynski, R., Mlynski, B., & Mlynski, G. (2005). Long-term rhinoflowmetry: A new method for functional rhinologic diagnostics. *American Journal of Rhinology*, 19(1), 53–57. <https://doi.org/10.1177/194589240501900109>
- Hahn, I., Scherer, P. W., & Mozell, M. M. (1993). Velocity profiles measured for airflow through a large-scale model of the human nasal cavity. *Journal of Applied Physiology*, 75(5), 2273–2287. <https://doi.org/10.1152/jappl.1993.75.5.2273>
- Hall, R. L. (2005). Energetics of nose and mouth breathing, body size, body composition, and nose volume in young adult males and females. *American Journal of Human*, 17(3), 321–330. <https://doi.org/10.1002/ajhb.20122>
- Hammer, Ø., Harper, D. A., & Ryan, P. D. (2001). PAST: Paleontological statistics software package for education and data analysis. *Palaeontologia Electronica*, 4(1), 9.
- Hanida, S., Mori, F., Kumahata, K., Watanabe, M., Ishikawa, S., & Matsuzawa, T. (2013). Influence of latent heat in the nasal cavity. *Journal of Biomechanical Science and Engineering*, 8(3), 209–224. <https://doi.org/10.1299/jbse.8.209>
- Harvati, K., & Weaver, T. D. (2006). Human cranial anatomy and the differential preservation of population history and climate signatures. *The Anatomical Record Part A: Discoveries in Molecular, Cellular, and Evolutionary Biology: An Official Publication of the American Association of Anatomists*, 288(12), 1225–1233. <https://doi.org/10.1002/ar.a.20395>
- Havenith, G. (2005). Temperature regulation, heat balance and climatic stress. In W. Kirch, R. Bertollini, & B. Menne (Eds.), *Extreme weather events and public health responses* (pp. 69–80). Springer-Verlag. [https://doi.org/10.1007/3-540-28862-7\\_7](https://doi.org/10.1007/3-540-28862-7_7)
- Heuzé, Y. (2019). What does nasal cavity size tell us about functional nasal airways? *Bulletins et Mémoires de la Société d'Anthropologie de Paris*, 31(1–2), 69–76. <https://doi.org/10.3166/bmsap-2018-0011>
- Holton, N., Yokley, T., & Butaric, L. (2013). The morphological interaction between the nasal cavity and maxillary sinuses in living humans. *The Anatomical Record*, 296(3), 414–426. <https://doi.org/10.1002/ar.22655>
- Holton, N. E., Alsamawi, A., Yokley, T. R., & Froehle, A. W. (2016). The ontogeny of nasal shape: An analysis of sexual dimorphism in a longitudinal sample. *American Journal of Physical Anthropology*, 160(1), 52–61. <https://doi.org/10.1002/ajpa.22941>
- Holton, N. E., Franciscus, R. G., Marshall, S. D., Southard, T. E., & Nieves, M. A. (2011). Nasal septal and premaxillary developmental integration: Implications for facial reduction in *Homo*. *The Anatomical Record*, 294(1), 68–78. <https://doi.org/10.1002/ar.21288>
- Holton, N. E., Yokley, T. R., & Figueroa, A. (2012). Nasal septal and craniofacial form in European-and African-derived populations. *Journal of Anatomy*, 221(3), 263–274. <https://doi.org/10.1111/j.1469-7580.2012.01533.x>
- Holton, N. E., Yokley, T. R., Froehle, A. W., & Southard, T. E. (2014). Ontogenetic scaling of the human nose in a longitudinal sample: Implications for genus *Homo* facial evolution. *American Journal of Physical Anthropology*, 153(1), 52–60. <https://doi.org/10.1002/ajpa.22402>
- Hopkins, C. (2021). Nose, nasal cavity and paranasal sinuses. In S. Standring (Ed.), *Gray's anatomy: The anatomical basis of clinical practice* (pp. 686–701). Elsevier Health Sciences.
- Hörschler, I., Schröder, W., & Meinke, M. (2010). On the assumption of steadiness of nasal cavity flow. *Journal of Biomechanics*, 43(6), 1081–1085. <https://doi.org/10.1016/j.jbiomech.2009.12.008>
- Ingelstedt, S., & Ivstam, B. (1951). Study in the humidifying capacity of the nose. *Acta Oto-Laryngologica*, 39(4), 286–290. <https://doi.org/10.3109/00016485109119255>
- Inthavong, K., Chetty, A., Shang, Y., & Tu, J. (2018). Examining mesh independence for flow dynamics in the human nasal cavity. *Computers in Biology and Medicine*, 102, 40–50. <https://doi.org/10.1016/j.combiomed.2018.09.010>
- Inthavong, K., Ma, J., Shang, Y., Dong, J., Chetty, A. S., Tu, J., & Franklto, D. (2019). Geometry and airflow dynamics analysis in the nasal cavity during inhalation. *Clinical Biomechanics*, 66, 97–106. <https://doi.org/10.1016/j.clinbiomech.2017.10.006>
- Inthavong, K., Tian, Z. F., & Tu, J. Y. (2007). CFD simulations on the heating capability in a human nasal cavity. In P. Jacobs, T. McIntyre, M. Cleary, D. Buttsworth, R. Mee, R. Clements, R. Morgan, & C. Lemckert (Eds.), *Proceedings of the 16th Australasian fluid mechanical conference (AFMC)* (pp. 842–847). School of Engineering, The University of Queensland.
- Inthavong, K., Wen, J., Tu, J., & Tian, Z. (2009). From CT scans to CFD modelling—fluid and heat transfer in a realistic human nasal cavity. *Engineering Applications of Computational Fluid Mechanics*, 3(3), 321–335. <https://doi.org/10.1080/19942060.2009.11015274>
- Jafek, B. W. (1983). Ultrastructure of human nasal mucosa. *Laryngoscope*, 93, 1576–1599. <https://doi.org/10.1288/00005537-198312000-00011>
- Keck, T., Leiacker, R., Heinrich, A., Kühnemann, S., & Rettinger, G. (2000). Humidity and temperature profile in the nasal cavity. *Rhinology*, 38(4), 167–171.
- Keck, T., Leiacker, R., Riechelmann, H., & Rettinger, G. (2000). Temperature profile in the nasal cavity. *The Laryngoscope*, 110(4), 651–654. <https://doi.org/10.1097/00005537-200004000-00021>
- Kelly, A. P., Ocobock, C., Butaric, L. N., & Maddux, S. D. (2023). Metabolic demands and sexual dimorphism in human nasal morphology: A test of the respiratory-energetics hypothesis. *American Journal of Biological Anthropology*, 180(3), 453–471. <https://doi.org/10.1002/ajpa.24692>
- Keustermans, W., Huysmans, T., Danckaers, F., Zarowski, A., Schmelzer, B., Sijbers, J., & Dirckx, J. J. (2018). High quality statistical shape modelling of the human nasal cavity and applications. *Royal Society Open Science*, 5(12), 181558. <https://doi.org/10.1098/rsos.181558>
- Keyhani, K., Scherer, P. W., & Mozell, M. M. (1995). Numerical simulation of airflow in the human nasal cavity. *Journal of Biomechanical Engineering*, 117, 429–441. <https://doi.org/10.1115/1.2794204>

- Kim, D. W., Chung, S.-K., & Na, Y. (2017). Numerical study on the air conditioning characteristics of the human nasal cavity. *Computers in Biology and Medicine*, 86, 18–30. <https://doi.org/10.1016/j.combiomed.2017.04.018>
- Kloss-Brandstätter, A., Summerer, M., Horst, D., Horst, B., Streiter, G., Raschenberger, J., Kronenberg, F., Sanguansermsri, T., Horst, J., & Weissensteiner, H. (2021). An in-depth analysis of the mitochondrial phylogenetic landscape of Cambodia. *Scientific Reports*, 11(1), 10816. <https://doi.org/10.1038/s41598-021-90145-2>
- Kumahata, K., Mori, F., Ishikawa, S., & Matsuzawa, T. (2010). Nasal flow simulation using heat and humidity models. *Journal of Biomechanical Science and Engineering*, 5(5), 565–577. <https://doi.org/10.1299/jbse.5.565>
- Lee, H. P., & Gordon, B. R. (2012). Impacts of fluid dynamics simulation in study of nasal airflow physiology and pathophysiology in realistic human three-dimensional nose models. *Clinical and Experimental Otorhinolaryngology*, 5(4), 181–187. <https://doi.org/10.3342/ceo.2012.5.4.181>
- Leonard, W. R., Snodgrass, J. J., & Sorensen, M. V. (2005). Metabolic adaptation in indigenous Siberian populations. *Annual Review of Anthropology*, 34, 451–471. <https://doi.org/10.1146/annurev.anthro.34.081804.120558>
- Lindemann, J., Brambs, H. J., Keck, T., Wiesmiller, K. M., Rettinger, G., & Pless, D. (2005). Numerical simulation of intranasal airflow after radical sinus surgery. *American Journal of Otolaryngology*, 26(3), 175–180. <https://doi.org/10.1016/j.amjoto.2005.02.010>
- Lindemann, J., Keck, T., Wiesmiller, K. M., Rettinger, G., Brambs, H. J., & Pless, D. (2005). Numerical simulation of intranasal air flow and temperature after resection of the turbinates. *Rhinology*, 43(1), 24–28.
- Lindemann, J., Leiacker, R., Rettinger, G., & Keck, T. (2002). Nasal mucosal temperature during respiration. *Clinical Otolaryngology & Allied Sciences*, 27(3), 135–139. <https://doi.org/10.1046/j.1365-2273.2002.00544.x>
- Maddux, S. D., Butaric, L. N., Yokley, T. R., & Franciscus, R. G. (2017). Ecogeographic variation across morphofunctional units of the human nose. *American Journal of Physical Anthropology*, 162(1), 103–119. <https://doi.org/10.1002/ajpa.23100>
- Maddux, S. D., Yokley, T. R., Svoma, B. M., & Franciscus, R. G. (2016). Absolute humidity and the human nose: A reanalysis of climate zones and their influence on nasal form and function. *American Journal of Physical Anthropology*, 161(2), 309–320. <https://doi.org/10.1002/ajpa.23032>
- Maréchal, L., Dumoncel, J., Santos, F., Astudillo Encina, W., Evteev, A., Prevost, A., Toro-Ibacache, V., Venter, R. G., & Heuzé, Y. (2023). New insights into the variability of upper airway morphology in modern humans. *Journal of Anatomy*, 242(5), 781–795. <https://doi.org/10.1111/joa.13813>
- Marks, T. N., Maddux, S. D., Butaric, L. N., & Franciscus, R. G. (2019). Climatic adaptation in human inferior nasal turbinate morphology: Evidence from Arctic and equatorial populations. *American Journal of Physical Anthropology*, 169(3), 498–512. <https://doi.org/10.1002/ajpa.23840>
- Maynard-Smith, J., Burian, R., Kauffman, S., Alberch, P., Campbell, J., Goodwin, B., Lande, R., Raup, D., & Wolpert, L. (1985). Developmental constraints and evolution. *The Quarterly Review of Biology*, 60(3), 265–287. <https://doi.org/10.1086/414425>
- McFadden, E. R., Jr., Pichurko, B. M., Bowman, H. F., Ingenito, E., Burns, S., Dowling, N., & Solway, J. (1985). Thermal mapping of the airways in humans. *Journal of Applied Physiology*, 58(2), 564–570. <https://doi.org/10.1152/jap.1985.58.2.564>
- Megía, I., Burgos, M. A., Sanmiguel Rojas, E., Torres-Tamayo, N., García-Martínez, D., Piqueras, F. M., & Bastir, M. (2018). Sexual dimorphism of nasal airways in modern humans. In C. Rissech, L. Lloveras, J. Nadal, & J. M. Fullola (Eds.), *Geometric morphometrics: Trends in biology, paleobiology and archaeology* (pp. 53–63). Seminari d'Estudis i Recerques Prehistòriques.
- Mlynski, G., Grützenmacher, S., Plontke, S., Mlynski, B., & Lang, C. (2001). Correlation of nasal morphology and respiratory function. *Rhinology*, 39(4), 197–201.
- Mori, F., Hanida, S., Kumahata, K., Miyabe-Nishiwaki, T., Suzuki, J., Matsuzawa, T., & Nishimura, T. D. (2015). Minor contributions of the maxillary sinus to the air-conditioning performance in macaque monkeys. *The Journal of Experimental Biology*, 218(15), 2394–2401. <https://doi.org/10.1242/jeb.118059>
- Naftali, S., Rosenfeld, M., Wolf, M., & Elad, D. (2005). The air-conditioning capacity of the human nose. *Annals of Biomedical Engineering*, 33, 545–553. <https://doi.org/10.1007/s10439-005-2513-4>
- Nishimura, T., Mori, F., Hanida, S., Kumahata, K., Ishikawa, S., Samarat, K., Miyabe-Nishiwaki, T., Hayashi, M., Tomonaga, M., Suzuki, J., Matsuzawa, T., & Matsuzawa, T. (2016). Impaired air conditioning within the nasal cavity in flat-faced *Homo*. *PLoS Computational Biology*, 12(3), e1004807. <https://doi.org/10.1371/journal.pcbi.1004807>
- Noback, M. L., Harvati, K., & Spoor, F. (2011). Climate-related variation of the human nasal cavity. *American Journal of Physical Anthropology*, 145(4), 599–614. <https://doi.org/10.1002/ajpa.21523>
- Ocobock, C., Soppela, P., Turunen, M., Stenbäck, V., & Herzig, K. H. (2022). Brown adipose tissue thermogenesis among a small sample of reindeer herders from sub-Arctic Finland. *Journal of Physiological Anthropology*, 41(1), 17. <https://doi.org/10.1186/s40101-022-00290-4>
- Ocobock, C., Soppela, P., Turunen, M., Stenbäck, V., Herzig, K. H., Rimbach, R., & Pontzer, H. (2021). Reindeer herders from subarctic Finland exhibit high total energy expenditure and low energy intake during the autumn herd roundup. *American Journal of Human Biology*, 34(4), e23676. <https://doi.org/10.1002/ajhb.23676>
- Patel, R. G., Garcia, G. J., Frank-Ito, D. O., Kimbell, J. S., & Rhee, J. S. (2015). Simulating the nasal cycle with computational fluid dynamics. *Otolaryngology-Head and Neck Surgery*, 152(2), 353–360. <https://doi.org/10.1177/0194599814559385>
- Proctor, D. F. (1977). The upper airways: I. Nasal physiology and defense of the lungs. *American Review of Respiratory Disease*, 115(1), 97–129. <https://doi.org/10.1164/arrd.1977.115.1.97>
- Proctor, D. F. (1987). The upper airways: Interface between the lungs and the ambient air. *American Journal of Rhinology*, 1(1), 27–32. <https://doi.org/10.2500/105065887781390354>
- Proctor, D. F., & Andersen, I. H. P. (1982). *The nose: Upper airway physiology and the atmospheric environment*. Elsevier Biomedical Press.
- Proetz, A. W. (1951). Air currents in the upper respiratory tract and their clinical importance. *The Annals of Otolaryngology, Rhinology, and Laryngology*, 60, 439–467. <https://doi.org/10.1177/000348945106000216>
- R Core Team. (2022). R: A language and environment for statistical computing [compute software]. Vienna: R Foundation for Statistical Computing. Retrieved from <https://www.R-project.org/>
- Ramprasad, V. H., & Frank-Ito, D. O. (2016). A computational analysis of nasal vestibule morphologic variabilities on nasal function. *Journal of Biomechanics*, 49(3), 450–457. <https://doi.org/10.1016/j.jbiomech.2016.01.009>
- Rosas, A., & Bastir, M. (2002). Thin-plate spline analysis of allometry and sexual dimorphism in the human craniofacial complex. *American Journal of Physical Anthropology*, 117(3), 236–245. <https://doi.org/10.1097/00005537-199909000-00027>
- Rouadi, P., Baroody, F. M., Abbott, D., Naureckas, E., Solway, J., & Naclerio, R. M. (1999). A technique to measure the ability of the human nose to warm and humidify air. *Journal of Applied Physiology*, 87(1), 400–406. <https://doi.org/10.1152/jap.1999.87.1.400>
- Sahin-Yilmaz, A., & Naclerio, R. M. (2011). Anatomy and physiology of the upper airway. *Proceedings of the American Thoracic Society*, 8(1), 31–39. <https://doi.org/10.1513/pats.201007-05ORN>
- Schlager, S., & Rüdell, A. (2015). Analysis of the human osseous nasal shape—Population differences and sexual dimorphism. *American Journal of Physical Anthropology*, 157(4), 571–581. <https://doi.org/10.1002/ajpa.22749>

- Schmidt-Nielsen, K., Hainsworth, F. R., & Murrish, D. E. (1970). Counter-current heat exchange in the respiratory passages: Effect on water and heat balance. *Respiration Physiology*, 9(2), 263–276. [https://doi.org/10.1016/0034-5687\(70\)90075-7](https://doi.org/10.1016/0034-5687(70)90075-7)
- Schroter, R. C., & Watkins, N. V. (1989). Respiratory heat exchange in mammals. *Respiration Physiology*, 78(3), 357–367. [https://doi.org/10.1016/0034-5687\(89\)90110-2](https://doi.org/10.1016/0034-5687(89)90110-2)
- Shah, R., & Frank-Ito, D. O. (2022). The role of normal nasal morphological variations from race and gender differences on respiratory physiology. *Respiratory Physiology & Neurobiology*, 297, 103823. <https://doi.org/10.1016/j.resp.2021.103823>
- Siu, J., Inthavong, K., Dong, J., Shang, Y., & Douglas, R. G. (2021). Nasal air conditioning following total inferior turbinectomy compared to inferior turbinoplasty—A computational fluid dynamics study. *Clinical Biomechanics*, 81, 105237. <https://doi.org/10.1016/j.clinbiomech.2020.105237>
- Snodgrass, J. J., Leonard, W. R., Tarskaia, L. A., Alekseev, V. P., & Krivoschapkin, V. G. (2005). Basal metabolic rate in the Yakut (Sakha) of Siberia. *American Journal of Human Biology*, 17(2), 155–172. <https://doi.org/10.1002/ajhb.20106>
- Taylor, D. J., Doorly, D. J., & Schroter, R. C. (2010). Inflow boundary profile prescription for numerical simulation of nasal airflow. *Journal of the Royal Society Interface*, 7(44), 515–527. <https://doi.org/10.1098/rsif.2009.0306>
- Thomson, A., & Buxton, L. D. (1923). Man's nasal index in relation to certain climatic conditions. *Journal of the Anthropological Institute of Great Britain and Ireland*, 53, 92–122. <https://doi.org/10.2307/2843753>
- Tomczak, M., & Tomczak, E. (2014). The need to report effect size estimates revisited. An overview of some recommended measures of effect size. *Trends in Sport Sciences*, 21(1), 19–25.
- Torres-Tamayo, N., García-Martínez, D., Lois Zolniski, S., Torres-Sánchez, I., García-Río, F., & Bastir, M. (2018). 3D analysis of sexual dimorphism in size, shape and breathing kinematics of human lungs. *Journal of Anatomy*, 232(2), 227–237. <https://doi.org/10.1111/joa.12743>
- Tran, C. N. H., & Schroeder, L. (2021). Common evolutionary patterns in the human nasal region across a worldwide sample. *American Journal of Physical Anthropology*, 176(3), 422–433. <https://doi.org/10.1002/ajpa.24378>
- Walker, J. E. C., Wells, R. E., & Merrill, E. W. (1961). Heat and water exchange in the respiratory tract. *The American Journal of Medicine*, 30, 259–267. [https://doi.org/10.1016/0002-9343\(61\)90097-3](https://doi.org/10.1016/0002-9343(61)90097-3)
- Webb, P. (1951). Air temperatures in respiratory tracts of resting subjects in cold. *Journal of Applied Physiology*, 4(5), 378–382. <https://doi.org/10.1152/jappl.1951.4.5.378>
- Weiner, J. S. (1954). Nose shape and climate. *American Journal of Physical Anthropology*, 12(4), 615–618. <https://doi.org/10.1002/ajpa.1330120412>
- Weinhold, I., & Mlynski, G. (2004). Numerical simulation of airflow in the human nose. *European Archives of Oto-Rhino-Laryngology and Head & Neck*, 261, 452–455. <https://doi.org/10.1007/s00405-003-0675-y>
- Wen, J., Inthavong, K., Tu, J., & Wang, S. (2008). Numerical simulations for detailed airflow dynamics in a human nasal cavity. *Respiratory Physiology & Neurobiology*, 161(2), 125–135. <https://doi.org/10.1016/j.resp.2008.01.012>
- White, M. D. (2006). Components and mechanisms of thermal hyperpnea. *Journal of Applied Physiology*, 101(2), 655–663. <https://doi.org/10.1152/jappphysiol.00210.2006>
- Wickham, H. (2016). *ggplot2: Elegant graphics for data analysis*. Springer-Verlag.
- Wolf, M., Naftali, S., Schroter, R. C., & Elad, D. (2004). Air-conditioning characteristics of the human nose. *The Journal of Laryngology and Otolaryngology*, 118, 87–92. <https://doi.org/10.1258/002221504772784504>
- Wroe, S., Parr, W. C., Ledogar, J. A., Bourke, J., Evans, S. P., Fiorenza, L., Benazzi, S., Hublin, J.-J., Stringer, C., Kullmer, O., Curry, M., Rae, T. C., & Yokley, T. R. (2018). Computer simulations show that Neanderthal facial morphology represents adaptation to cold and high energy demands, but not heavy biting. *Proceedings of the Royal Society B: Biological Sciences*, 285(1876), 20180085. <https://doi.org/10.1098/rspb.2018.0085>
- Xiong, G. X., Zhan, J. M., Jiang, H. Y., Li, J. F., Rong, L. W., & Xu, G. (2008). Computational fluid dynamics simulation of airflow in the normal nasal cavity and paranasal sinuses. *American Journal of Rhinology*, 22(5), 477–482. <https://doi.org/10.2500/ajr.2008.22.3211>
- Yokley, T. R. (2009). Ecogeographic variation in human nasal passages. *American Journal of Physical Anthropology*, 138(1), 11–22. <https://doi.org/10.1002/ajpa.20893>
- Zaidi, A. A., Mattern, B. C., Claes, P., McEcoy, B., Hughes, C., & Shriver, M. D. (2017). Investigating the case of human nose shape and climate adaptation. *PLoS Genetics*, 13(3), e1006616. <https://doi.org/10.1371/journal.pgen.1006616>
- Zhao, K., & Jiang, J. (2014). What is normal nasal airflow? A computational study of 22 healthy adults. *International Forum of Allergy & Rhinology*, 4(6), 435–446. <https://doi.org/10.1002/alr.21319>
- Zhu, J. H., Lee, H. P., Lim, K. M., & Lee, S. J. (2011). Evaluation and comparison of nasal airway flow patterns among three subjects from Caucasian, Chinese and Indian ethnic groups using computational fluid dynamics simulation. *Respiratory Physiology & Neurobiology*, 175(1), 62–69. <https://doi.org/10.1016/j.resp.2010.09.008>

## SUPPORTING INFORMATION

Additional supporting information can be found online in the Supporting Information section at the end of this article.

**How to cite this article:** Bastir, M., Sanz-Prieto, D., Burgos, M. A., Pérez-Ramos, A., Heuzé, Y., Maréchal, L., Evteev, A., Toro-Ibacache, V., & Esteban-Ortega, F. (2024). Beyond skeletal studies: A computational analysis of nasal airway function in climate adaptation. *American Journal of Biological Anthropology*, e24932. <https://doi.org/10.1002/ajpa.24932>